

HYDROTHERMAL ALTERATION AND METAMORPHISM  
OF A METADIABASE SILL,  
LAKE MICHIGANME, NORTHERN MICHIGAN.

A THESIS  
SUBMITTED TO THE FACULTY OF THE GRADUATE SCHOOL  
OF THE UNIVERSITY OF MINNESOTA

BY  
INGRID JOYCE VERHAGEN

IN PARTIAL FULFILLMENT OF THE REQUIREMENTS  
FOR THE DEGREE OF  
MASTER OF SCIENCE  
JUNE 1985

## ABSTRACT

The study area is at the western end of the Marquette synclinorium which developed during the Early Proterozoic. In the area, the stratigraphy of the northern limb of the synclinorium from north to south is Siamo Slate, Negaunee Iron-Formation, and Goodrich Quartzite. The sill intruded the iron-formation and separates the iron-formation from the slate in the northern part of the area whereas it separates the iron-formation from the quartzite in the southern part of the area. Large euhedral crystals of varying mineralogy especially almandine and grunerite and abundant chlorite are developed between the Negaunee Iron-Formation and a metadiabase sill at the Michigamme Mine (at the center of the area) in a chlorite schist. This study was undertaken to determine what caused chlorite to develop between the lithologies and whether it occurred before or after regional metamorphism (1.8 to 1.9 b.y.) which produced the large crystals at the mine.

Petrographic examination of the metadiabase sill and the Negaunee Iron-Formation indicates that the chlorite was developed before the large crystals of almandine and grunerite. The Negaunee Iron-Formation contains an assemblage of quartz- magnetite- almandine- chlorite- grunerite- stilpnomelane. It is commonly brecciated and separated from the chlorite schist by a layer of almandine. The metadiabase is divided into four zones, from the center of the sill to the margins, dependent on the amount of chlorite in the rock and the presence of relict poikilitic texture. A relict poikilitic texture of labradorite and augite located in Zone 1 can be correlated to a relict poikilitic texture of plagioclase and hornblende which is present from Zone 2 through Zone 3A of the sill. Almandine, in Zone 3B, developed after chloritized hornblende. Zone 4 contains the most-altered sill which is predominantly a chlorite schist. The chlorite schist contains an ellipsoidal texture which can be traced from Zone 3B of the metadiabase and the same

mineralogy as the iron-formation but in very different proportions. The ellipsoidal texture developed prior to the growth of almandine and grunerite.

Whole rock chemical analysis was carried out on eleven samples across the metadiabase sill towards its upper margin which is in contact with the Negaunee Iron- Formation. These samples document the major element changes occurring in the sill through its four zones. The behavior of the major elements across the sill is comparable to the behavior of major elements in several seawater alteration (hydrothermal) suites (Mottl, 1983; Miyashiro, 1979). <sup>\*</sup> FeO (total iron as FeO) and MgO increase while  $\text{SiO}_2$ , CaO, and  $\text{Na}_2\text{O}$  all decrease in abundance with increasing degree of alteration. The hydrothermal fluids probably percolated through the Negaunee Iron- Formation where iron was leached. This aided in a major chemical exchange between calcium from the diabase and iron (or magnesium) from the altering fluid which may have been similar to seawater. Chlorite was probably developed as a result of this exchange at  $300^\circ\text{C}$  in a strongly fluid-dominated system (Mottl, 1983).

The metadiabase, iron-formation, and chlorite schist are related on a CFM diagram (Abbott, 1982). This diagram shows that the equilibrium assemblages in the sill are dependent on the bulk composition of the sill which varies from Zone 1 to Zone 4. Assemblages containing almandine are restricted to calcium-depleted and iron-enriched areas of the sill. The depletion of calcium and enrichment of iron moves the bulk compositions of the sill closer to the bulk compositions of the iron- formation and the link between the compositions of these two lithologies is the most-altered metadiabase (the chlorite schist). The compositional dependence of the assemblages suggests that hydrothermal alteration preceded regional metamorphism.

## ACKNOWLEDGMENTS

I would like to thank several individuals for their contribution to this thesis. First, my advisor, Dr. J.A. Grant who suggested the project and whose continued interest benefitted the thesis.

William Kangas and Cleveland Cliffs Iron Company of Ishpeming, Michigan graciously allowed access to drill core and data of drill core around the Michigamme Mine.

Drs. S.D. McDowell and T.J. Bornhorst of Michigan Technological University carried out chemical analysis on several important samples.

Drs. B.P. Tsai and J.C. Green served on the thesis committee and provided constructive criticism of the thesis.

The Department of Geology provided financial assistance for field work during the summer of 1983.

Finally, I would like to thank my family, friends, and fellow graduate students whose encouragement kept me motivated.

TABLE OF CONTENTS

|                                  | <u>Page</u> |
|----------------------------------|-------------|
| ABSTRACT . . . . .               | i           |
| ACKNOWLEDGMENTS. . . . .         | iii         |
| TABLE OF CONTENTS. . . . .       | iv          |
| ILLUSTRATIONS. . . . .           | vi          |
| TABLES . . . . .                 | viii        |
| PLATES . . . . .                 | ix          |
| INTRODUCTION . . . . .           | 1           |
| GEOLOGIC SETTING . . . . .       | 1           |
| STATEMENT OF PROBLEM . . . . .   | 4           |
| METHOD OF STUDY. . . . .         | 6           |
| PREVIOUS WORK. . . . .           | 7           |
| FIELD RELATIONSHIPS. . . . .     | 9           |
| PETROGRAPHY. . . . .             | 17          |
| SIAMO SLATE. . . . .             | 17          |
| NEGAUNEE IRON FORMATION. . . . . | 17          |
| GOODRICH ARGILLITE . . . . .     | 21          |
| METADIABASE. . . . .             | 21          |
| Zone 1. . . . .                  | 22          |
| Zone 2. . . . .                  | 25          |
| Zone 3A . . . . .                | 29          |
| Zone 3B . . . . .                | 30          |
| Zone 4 . . . . .                 | 34          |
| Biotite Schist . . . . .         | 34          |

|  |    |
|--|----|
| Chlorite Schist. . . . .                             | 37 |
| Chlorite Schist-Negaunee Iron-Formation Contact      | 41 |
| Summary . . . . .                                    | 43 |
| CHEMICAL ANALYSIS. . . . .                           | 46 |
| COMPARISON WITH MODERN HYDROTHERMAL SYSTEMS. . . . . | 53 |
| SUMMARY. . . . .                                     | 60 |
| INTERPRETATION . . . . .                             | 61 |
| SCENARIO . . . . .                                   | 74 |
| SUMMARY AND CONCLUSIONS. . . . .                     | 76 |
| REFERENCES . . . . .                                 | 79 |
| APPENDIX . . . . .                                   | A1 |

ILLUSTRATIONS

| <u>FIGURE</u>   | <u>Page</u> |
|---|-------------|
| 1. Location map of the study area . . . . .   | 2           |
| 2. Waste sample at Michigamme Mine. . . . .   | 5           |
| 3. Outcrop of Negaunee Iron-Formation, south of Michigamme Methodist Institute . . . . .                                      | 5           |
| 4. Large concentration of chloritoid in the schist of the Goodrich Quartzite, on the north shore of Lake Michigamme . . . . . | 11          |
| 5. Outcrop of metadiabase sill, south of Michigamme Methodist Institute. . . . .  | 11          |
| 6. Weathered plagioclase laths on surface of metadiabase, north of Michigamme Mine. . . . .                                   | 13          |
| 7. Milky quartz layer on metadiabase, south of Middle Lake . . . . .  | 13          |
| 8. Lithologic sequence of DDH 4 at contact of chlorite schist and Negaunee Iron-Formation.                                    | 15          |
| 9. Photomicrograph of euhedral garnet over fibrous grunerite. . . . .   | 19          |
| 10. Photomicrograph of poikilitic intergrowth of plagioclase and augite . . . . .   | 19          |
| 11. Photomicrograph and sketch of boundary outline of plagioclase laths preserved within hornblende. . . . .                  | 27          |
| 12. Photomicrograph of aggregate quartz after hornblende. . . . .   | 28          |
| 13. Photomicrograph of chlorite replacing plagioclase along boundaries . . . . .  | 28          |
| 14. Photomicrograph of quartz rimmed by fine-grained quartz . . . . .   | 31          |
| 15. Photomicrograph of hornblende with chlorite along cleavage . . . . .  | 31          |
| 16. Photomicrograph and sketch of chlorite pseudomorph after andesine . . . . .   | 33          |

FIGURE

|   |    |
|---|----|
| 17. Photomicrograph of euhedral garnet adjacent to chlorite pseudomorph after hornblende . . . . .                                      | 35 |
| 18. Photomicrograph of calcite and hematite pseudomorph after hornblende . . . . .  | 36 |
| 19. Photomicrograph of ellipsoid of fine-grained chlorite outlined by magnetite, biotite, and quartz . . . . .                          | 38 |
| 20. Photomicrograph of chlorite pseudomorph after plagioclase . . . . .   | 38 |
| 21. Photomicrograph of aggregate quartz within distorted tabular area replaced by biotite and chlorite along boundary of area . . . . . | 40 |
| 22. Photomicrograph of grunerite rimmed by chlorite and quartz . . . . .  | 40 |
| 23. Photomicrograph and sketch of chlorite ellipsoids   | 42 |
| 24. Photomicrograph of brecciated iron-formation .  | 44 |
| 25. Photomicrograph of almandine layer separating iron-formation from chlorite schist. . . . .  | 44 |
| 26. Graph of rare-earth elements normalized to chondrites versus atomic number . . . . .  | 52 |
| 27. Graph of trace element concentration versus distance across the sill towards its upper margin . . . . .                             | 54 |
| 28. Graph of trace element concentration versus distance across the sill towards its upper margin . . . . .                             | 54 |
| 29. Model predicting the mineral assemblages and proportions with varying sea water to rock ratios (Mottl, 1983). . . . .               | 58 |
| 30. Visual representation of mineral assemblages and proportions across the zones of the sill. . . . .                                  | 59 |
| 31. CFM diagram showing position of minerals from the metadiabase sill and the Negaunee Iron-Formation . . . . .                        | 64 |



FIGURE

|   |    |
|---|----|
| 32. Equilibrium assemblages of the metadiabase sill and bulk compositions plotted on the CFM diagram. . | 67 |
| 33. Equilibrium assemblages of the Negaunee Iron-Formation plotted on the CFM diagram. . . . .          | 71 |
| 34. Composition of minerals at Michigamme Mine (adapted from Haase, 1982) . . . . .                     | 72 |
| 35. Equilibrium assemblages of the Negaunee Iron-Formation . . . . .                                    | 73 |

TABLES

| <u>TABLE</u>   | <u>Page</u> |
|--|-------------|
| 1. Modal analyses of selected samples across the metadiabase sill . . . . .                                | 22          |
| 2. A: Composition of selected samples across the metadiabase toward the upper margin of the sill . . . . . | 47          |
| B: Table 2 from Mottl (p. 166). . . . .  | 48          |
| C: Table 1 from Miyashiro (p. M47) . . . . .   | 49          |
| 3. Trace elements for selected samples across the metadiabase toward the upper margin of the sill. . . . . | 50          |
| 4. Mineral formulas for the metadiabase and the Negaunee Iron-Formation . . . . .                          | 63          |
| 5-A. Equilibrium assemblages in the metadiabase. .   | 65          |
| 5-B. Equilibrium assemblages in the iron-formation   | 66          |
| 6. Estimation of modes of selected samples from the Negaunee Iron-Formation . . . . .                      | 70          |

PLATES

PLATE

Page

1. Geologic map of the study area, Northern Michigan. . . . . in back pocket
2. Sample location and outcrop map of the study area, Northern Michigan--Five parts . . in back pocket

## INTRODUCTION

An area of unusual metamorphism is found north of Lake Michigamme in northern Michigan. Large euhedral crystals (reaching several cm in diameter) and striking assemblages of chlorite -garnet -grunerite -magnetite -quartz are developed at the contact of the metadiabase sill and the Negaunee Iron- Formation. These combinations suggest that chemical interactions occurred between the two lithologies.

Field relationships, petrography, and chemical analysis were utilized to unravel the sequence of metamorphism which produced the mineral assemblages found in the area. Two metamorphic events left their imprint on the rocks and they will be discussed along with the chemical interactions which created the observed mineralogy.

### GEOLOGIC SETTING

The central northern peninsula of Michigan provides the setting for the study area which is divided equally between Baraga and Marquette counties (Figure 1). The area is located at the western end of the Marquette trough and restricted to its northern limb. The Marquette trough is a fault-bounded basin (graben) developed during the Early Proterozoic which is about 1,000 meters deep and 10 km wide in the Lake Michigamme area (Klasner and Cannon, 1974). The general stratigraphy from north to south (oldest to youngest) is Archaean gneiss, Menominee Group, and Baraga Group. These predate the intrusion of a metadiabase sill and dikes. Both groups of sediments indicate deposition in an actively subsiding basin during the Early Proterozoic. The Siamo Slate and Negaunee Iron- Formation are part of the Menominee Group while the

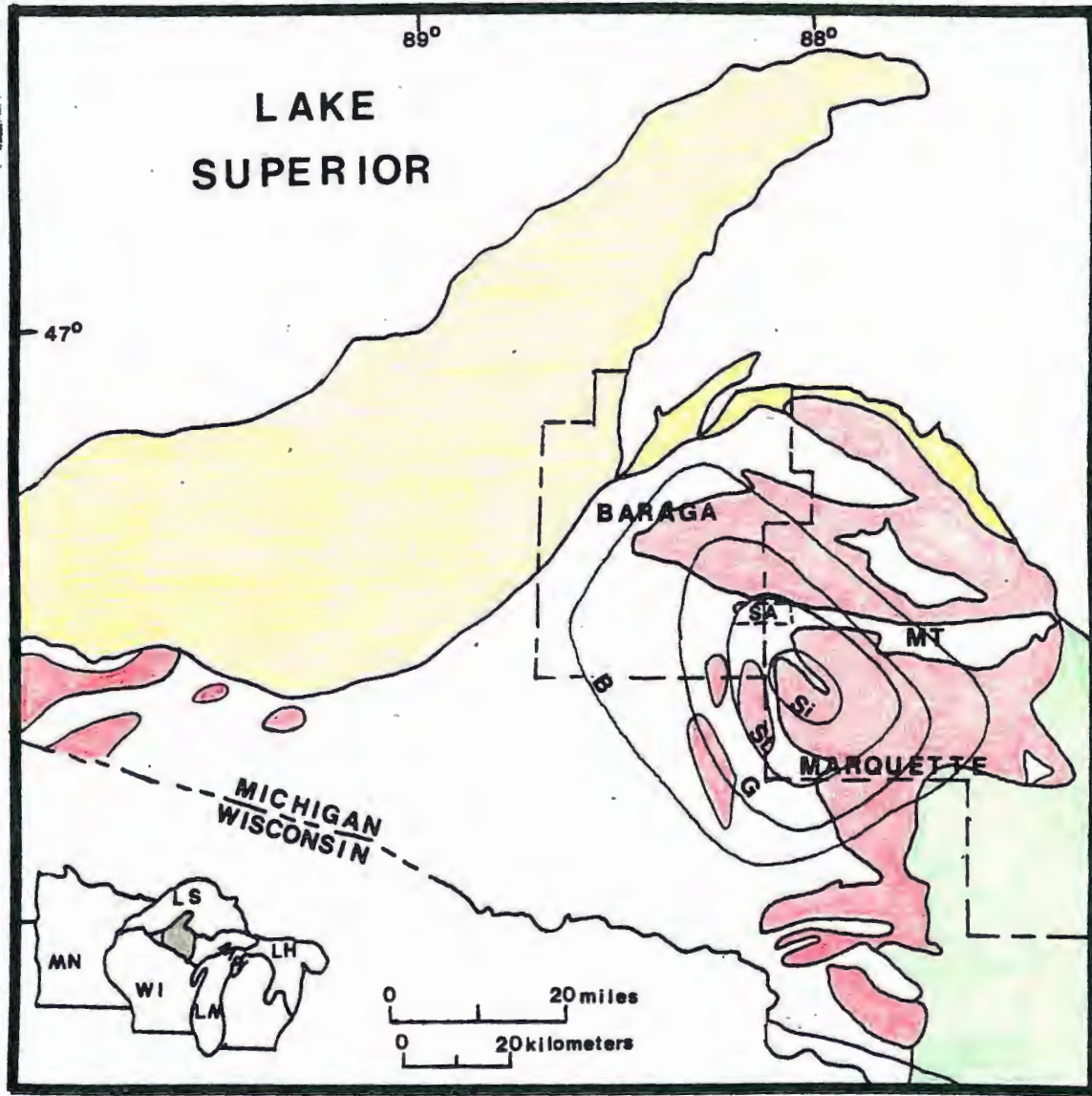


FIGURE 1: Location map showing study area with respect to regional geology. Adapted from Klasner and Cannon, 1972. Explanation of symbols used given on following page.

EXPLANATION



PALEOZOIC ROCKS



MIDDLE TO LATE PROTEROZOIC ROCKS (KEWEENAWAN)  
(PRECAMBRIAN Y).



EARLY PROTEROZOIC ROCKS (PRECAMBRIAN X).



ARCHEAN ROCKS (PRECAMBRIAN W).

B

BIOTITE ISOGRAD

G

GARNET ISOGRAD

St

STAUROLITE ISOGRAD

Si

SILLIMANITE ISOGRAD

SA

STUDY AREA

MT

MARQUETTE TROUGH

LH

LAKE HURON

LM

LAKE MICHIGAN

LS

LAKE SUPERIOR

MI

MICHIGAN

MN

MINNESOTA

WI

WISCONSIN

Goodrich Quartzite is near the base of the Baraga Group. Emplacement of the sill occurred prior to development of the Marquette trough because it is folded with the adjacent sediments (Cannon and Klasner, 1974).

Annular nodes of metamorphism delineated by regional metamorphic isograds are found throughout northern Michigan (James, 1955), as a result of the Middle Proterozoic Penokean Orogeny (1.8 - 1.9 b.y. before present). The isograds range from the biotite isograd on the outside of the nodes up to the sillimanite isograd in their centers. The study area is part of the Republic node within the staurolite isograd (Figure 1).

The northern limb of the trough is cut by several strike-slip faults which developed during the Middle Proterozoic. These north-trending faults have not been affected by Penokean deformation (Cannon and Klasner, 1972).

#### STATEMENT OF PROBLEM

An enigmatic chlorite schist is found in waste samples at the Michigamme Mine (Plate 1). Randomly - oriented grunerite blades and magnetite octahedra are set in a matrix of chlorite. The schist is commonly separated from the Negaunee Iron-Formation by a layer of almandine (Figure 2).

Several questions arise from examining the schist samples. First, what was the protolith of the chlorite schist? Second, what caused the formation of abundant chlorite adjacent to the Negaunee Iron Formation within an area of medium- to high-grade regional metamorphism (amphibolite facies)? Third, what caused a layer of almandine to

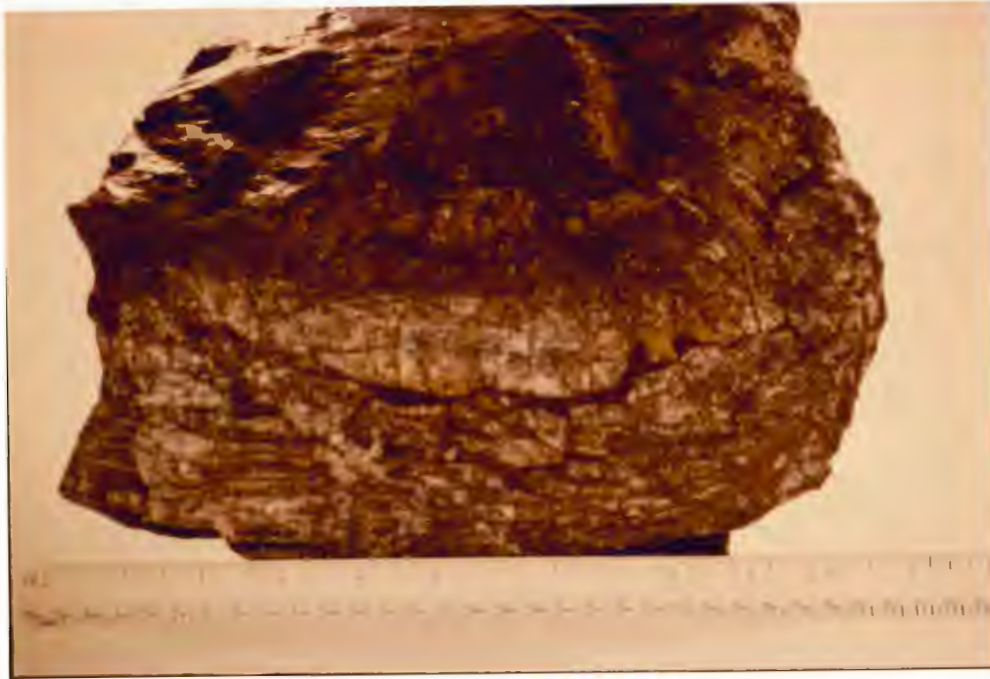


FIGURE 2: Waste sample collected at Michigamme Mine. Chlorite schist (top) is separated from brecciated iron-formation by a layer of garnet. Scale is in inches.



FIGURE 3: Outcrop of Negaunee Iron-Formation, south of Michigamme Methodist Institute. Three joint sets are shown. 1"=1 ft.

develop between the schist and the iron formation? Finally, what is the lateral distribution of the chlorite schist? The purpose of this study is to answer these questions.

#### METHOD OF STUDY

Methods utilized in this study included extensive sampling across the strike of the formations, sampling and describing three drill holes near the Michigamme Mine, qualitative and quantitative examination of thin sections, and chemical analysis of select samples across the sill.

Field work was completed during June and August of 1983. The base map used was by Klasner and Cannon (1978) and was expanded to a scale of 1:12,000. All outcrops sampled were located with the base map. The locations of the samples collected were determined by pace and compass and triangulating from prominent landmarks. Ten sample traverses (Plates 2-I through V) were taken across the strike of the formations. The location of the traverses were determined by noting the largest exposures of the sill, on the base map, as well as outcrops where the sill was in contact with the adjacent formations especially the iron-formation.

Drill core examination occurred in September of 1983 at Cleveland Cliffs Iron Company in Ishpeming, Michigan. Drill holes 4, 5, 6, taken from Section 19, T. 48 N., R. 31 W. (see Plate 2-IV), were described and logged. Samples were taken where major mineralogical changes occurred and where the sill was in contact with the iron-formation.

130 thin sections of the sill, iron-formation, and adjacent rock formations were examined qualitatively and semi-quantitatively (visual



estimation of modes). Samples from the sill analyzed by XRF were point-counted ( $> 300$  points per thin section).

The composition of plagioclase was determined by both the Michel Levy method and Carlsbad method.

Finally, select samples across the sill toward its contact with the iron-formation were analyzed by XRF at Michigan Technological University in Houghton, Michigan. Samples were taken from the southern (upper) margin of the sill where they are most-altered in texture and mineralogy. These samples were compared with the least-altered diabase in the center of the sill.

#### PREVIOUS WORK

Klasner and Cannon (1978) published the most recent map of the study area. Stratigraphic descriptions of the rock formations in adjacent quadrangles (Gair and Thaden, 1968; Gair, 1975) are applicable to their occurrence in the Michigamme area. A good synopsis of the geology of the western part of the Marquette trough is given by Cannon and Klasner (1972). The Negaunee Iron-Formation has been extensively studied while the chlorite schist and metadiabase sill have been only generally described. Four authors have discussed the chlorite schist to varying degrees.

H.L. James (1955) commented on the chlorite schist in his classical paper on the zones of regional metamorphism in northern Michigan.

"Dark-colored chloritic rocks, apparently sills, occur at Spurr Mine and adjacent properties on the north side of Lake Michigamme. Some of the rock contains large, well-formed partly chloritized garnets, up to an inch in diameter, in a matrix of chlorite. The chlorite probably is of retrograde origin."

Cannon and Klasner (1972) suggest that the altered mafic rocks at the Michigamme Mine "occur either as thin stringers intercalated with the iron formation, or as border zones, a foot or two thick on larger mafic bodies." Their unusual composition is attributed to "chemical interchange between the iron-formation and intrusive rocks either during emplacement or during later regional metamorphism."

J.E. Gair (1975) studied the geology of the Palmer Quadrangle (Marquette County) which is predominantly within a greenschist facies terrane. Gair noted the presence of "green to light -colored [dike] rock rich in chlorite, sericite, or clay." Diabasic texture was destroyed in thin mafic dikes or sills (less than 10 feet thick). He believed this was accomplished by plagioclase being either saussuritized, albitized, or replaced by a combination of calcite, quartz, chlorite, and biotite. Pyroxene was replaced by tremolite/actinolite or chlorite and biotite. Gair noted that the dikes were more altered where they cut the iron-formation. Reactants were derived from the iron-formation during emplacement and account for the breakdown of minerals in the dikes. Clastic lenses in the iron formation were chloritized where in contact with the dike; in these, magnetite was replaced by chlorite suggesting the iron-formation was also affected by the dike.

Finally, according to Gair (1975), "highly altered dike" was enriched in  $Al_2O_3$  and  $K_2O$  and depleted in  $FeO$ ,  $MgO$ ,  $CaO$ , and  $Na_2O$  while "chloritic dikes" were depleted in  $SiO_2$  and  $CaO$  as shown by chemical analysis.

Previous studies suggest that the protolith of the schist was a diabase. The studies do not address why abundant chlorite is present. This study sets out to determine what caused the development of chlorite and when it occurred.

#### FIELD RELATIONSHIPS

The study area encompasses approximately 6 square miles. The northwest corner of the field area is bounded by Trout, Middle, and Coon Lakes. Lake Michigamme bounds the southeast corner of the area. Three inactive iron-ore mines (Steward, Spurr, and Michigamme) are also found in the area and their waste piles are easily accessible from U.S. 41--M-28 which runs approximately east-west through the area. The Baraga-- Marquette County line is in the center of the study area. Good outcrop exposure for the formations studied is found south of Michigamme Methodist Institute on the northeast shore of Lake Michigamme (see Plate 1). Only the Negaunee Iron-Formation, metadiabase, and directly adjacent formations will be discussed in detail here. For a regional overview, James (1955) and Klasner (1978) provide information on the other rock formations in the Lake Michigamme area.

All the formations dip south and strike approximately east-west with the succession from north to south, prior to the intrusion of the sill, being the Siamo Slate, the Negaunee Iron-Formation, and the Goodrich Quartzite. The Siamo Slate and the Goodrich Quartzite were studied briefly to see if their mineralogy and grain size changed noticeably in approaching the contact with either the Negaunee Iron-Formation or the metadiabase sill. The sill intrudes the iron formation

at its base and isolates it from the slate in the northern part of the area. In the southern part of the field area, the sill intrudes into the upper section of the iron formation and separates the iron formation from the quartzite. The spatial relationships between the formations are complicated by several north-south trending strike-slip faults adjacent to the iron-ore mines. Displacement by these faults is seen in the Archean gneiss (north of the study area).

Outcrops of the Siamo Slate have a blocky appearance due to the combination of jointing which strikes N 15° W and dips 35° NE and bedding which strikes N 15° W and dips 55° SW. Weathering accentuates relict bedding but otherwise the rock is a fine-grained, gray-green phyllite.

The Negaunee Iron-Formation is poorly exposed but there are numerous prospect pits scattered throughout the area. The outcrops are small, blocky, southerly-dipping and vary in dimension from a meter to tens of meters in length. The Negaunee Iron-Formation crops out at lower elevations than the metadiabase. Three joint sets intersect at approximately right angles, as seen near Michigamme Methodist Institute, giving outcrops of the iron-formation a blocky appearance (Figure 3). The iron-formation easily breaks along bedding planes and this weakness allowed intrusion of the metadiabase. Where banding is not obscured by surficial oxidation, the iron-formation alternates between a matte burgundy and steel gray color due to the presence of hematite and magnetite, respectively.

The Goodrich Quartzite consists of a basal quartzite and an upper



FIGURE 4: Large concentration of chloritoid (at the tip of the pencil) in a schist of the Goodrich Quartzite, on the north shore of Lake Michigamme.

FIGURE 5: Outcrop of metadiabase sill, south of Michigamme Methodist Institute. 1"=6'.



argillaceous schist which represents only a small portion of the formation. The quartzite is gray and nearly pure (Klasner and Cannon, 1978). The schist is found southwest of the Michigamme Methodist Institute. At the northern boundary of this small schist outcrop, large black chloritoid and partially pseudomorphed tabular chloritoid crystals are highly concentrated (Figure 4). The chloritoid reaches lengths of 5.0 cm and is weathered to off-white crystals standing out in the gray-green schist. The schist contains fine-grained, six-sided crystals of tourmaline in a chlorite-sericite matrix.

The metadiabase sill is approximately 300 meters wide across strike and is discontinuous along strike. The metadiabase is the topographic high in the area, and forms massive, vertical, segmented ridges with talus slopes along the margins (Figure 5). Jointing is locally parallel to strike and vertical. The metadiabase is a black to gray-green rock, with lath-shaped surficial pits resulting from the weathering out of plagioclase (Figure 6). Coarse-grained hornblende (1.5 cm in length) is visible on the outcrop surface and is randomly oriented. A poikiloblastic texture is seen locally with fine-grained plagioclase laths set in coarse-grained hornblende. At the margins of the metadiabase the hornblende is fine-grained (0.5 mm) and has a slight preferred orientation parallel to strike. A discontinuous milky quartz layer is found on a northerly-dipping fracture surface of the metadiabase at the upper margin of the sill south of Middle Lake (Figure 7).

At the margins of the sill, the metadiabase is represented by



FIGURE 6: Weathered plagioclase laths (white) on surface of metadiabase, north of Michigamme Mine.



FIGURE 7: Milky quartz layer on metadiabase, south of Middle Lake. Roadcut on south side of Hwy. 41. 1"=1 ft.

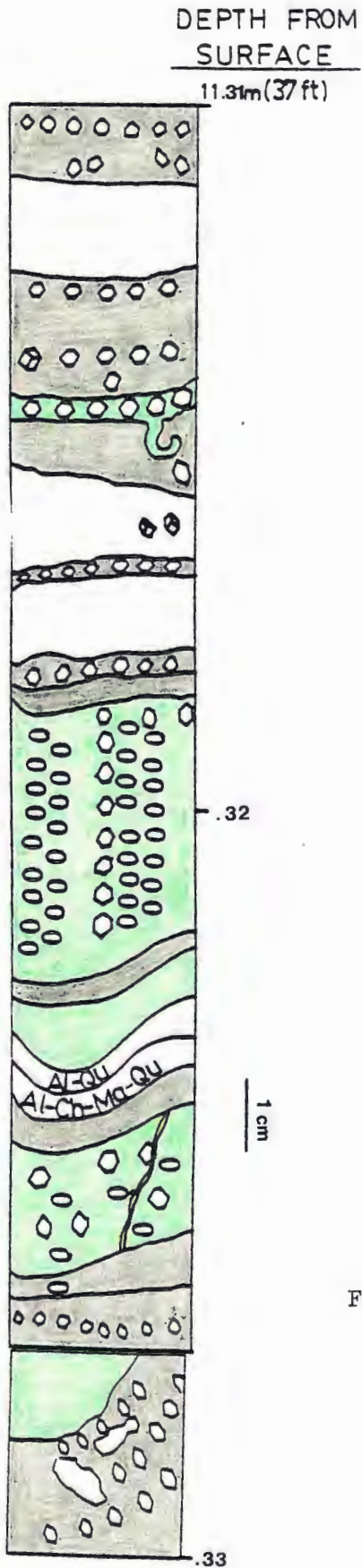
either a fine-grained, biotite-rich schist or a chlorite schist. The biotite schist is present at both margins of the sill and has been found southwest of the Michigamme Methodist Institute along the northern shore of Lake Michigamme, and also west of the Baraga-Marquette County line. The biotite schist outcrops are small bodies found at lower elevations than the metadiabase ridges. The biotite schist is adjacent to the Negaunee Iron-Formation but the contact is not exposed.

The chlorite schist locally crops out across from Townsend Ely Roadside Park (TERP) and at a roadcut between the Spurr and Steward Mines. It is restricted to the southern (upper) margin of the metadiabase. The outcrops are foliated, small, and rounded rising 1.5 to 3.0 meters above the surrounding surface and laterally extending for about 6.0 meters. The outcrops are isolated from the other formations and are weathered to a gray-green color but the rock is black on fresh surfaces.

The contact between the metadiabase and Siamo Slate crops out at several locations including southwest of Middle Lake, south of Coon Lake, and northeast of TERP. The contact northeast of TERP is the best example of the field relations between these two rocks and is found on the northern side of the ridge. Both the slate and the sill are massive units that are resistant to weathering. Quartz veins are present near the contact as well as subhedral pyrite grains.

A direct contact between the Negaunee Iron-Formation and the metadiabase does not crop out but is found in drill core and is seen in samples at the Michigamme Mine dumps. Direct contacts are found between





**LEGEND**

- ◊ Almandine porphyroblasts
- Al=almandine
- Ch=chlorite
- chlorite ellipsoids
- chlorite
- magnetite
- Ma=magnetite
- ⊗ pyrite
- Qu=quartz
- recrystallized quartz
- stilpnomelane

FIGURE 8: Lithologic sequence of DDH 4 at the contact between the Negaunee Iron-Formation and metadiabase sill.

the iron-formation and the sill in Diamond Drill Holes (DDHs) 4, 5, 6 (Cleveland Cliffs Iron Company) adjacent to the Michigamme Mine. In DDH 4 intercalation of the iron formation and the sill occurs at the contact of the two lithologies (Figure 8). Thinly-laminated to very thinly-bedded sugary quartz and magnetite of the iron formation alternate with layers of chlorite schist which flares locally into the iron-formation.

Samples from large waste piles at the Michigamme Mine display the spectacular relationships between the chlorite schist and the iron-formation which occur at their contact. These two lithologies are separated by a layer of garnet that is 2 cm thick. The iron-formation here has alternating layers of grunerite rosettes, sugary quartz, and magnetite, and is commonly brecciated. The chlorite schist contains randomly oriented blades of grunerite and dodecahedra of garnet (some up to 2 cm in diameter). Locally the garnet is pseudomorphed by chlorite. Magnetite octahedra (2 mm diameter) are dispersed throughout both rocks.

To summarize, the stratigraphy from north to south is the Siamo Slate, the Negaunee Iron-Formation, and the Goodrich Quartzite. The rock formations dip south. The sill appears to have intruded along bedding (a zone of weakness) in the iron formation and is found in contact with the slate in the northern part of the field area and the quartzite in the southern part of the field area. The metadiabase sill is the topographic high in the area. The margins of the sill are finer-grained than the core, are laced with abundant quartz veins, and are foliated parallel to strike.

## PETROGRAPHY

### SIAMO SLATE

The Siamo Slate is commonly a gray-green phyllite but locally a fine-grained, dark gray and off-white thinly-bedded feldspathic quartzite with appreciable clay matrix.

A brief petrographic examination was undertaken on the quartzite. Planar lamination is visible in thin section. The quartzite contains plagioclase feldspar and quartz. A few laminae consist of chlorite. Anhedronal plagioclase and quartz are replaced partially by sericite, biotite, and epidote. Subhedronal biotite alters to either chlorite or magnetite along cleavage planes. It is absent at the metadiabase contact where coarse-grained magnetite is present. Anhedronal epidote is present locally at the metadiabase contact. Calcite appears uncommonly as a late-stage mineral which crosscuts the other minerals.

The quartzite exhibits relatively constant grain size and mineralogy regardless of its distance from the contact with the sill. Distortion of bedding is uncommon but is linked to the increasing abundance of chlorite at certain locations (NI-6, Plate 2-III).

### NEGAUNEE IRON-FORMATION

The most widespread assemblage in the Negaunee Iron-Formation throughout the area is quartz- magnetite- almandine- chlorite- grunerite- stilpnomelane. Iron-formation containing this assemblage is in contact with the chlorite schist and the Goodrich Quartzite. Minor constituents are ankerite, apatite, biotite, hornblende, pyrite,

and minnesotaite. On the northern shore of Lake Michigan (south of TERP), minor amounts of muscovite and hematite are found.

In hand specimen, the rock varies from a thinly bedded to thickly laminated, fine-grained banded iron-formation. It commonly alternates between a chalk-gray and steel-gray color due to quartz and magnetite respectively. The presence of hematite at a few locations gives the rock a burgundy color. Brecciation of the bands is common in areas adjacent to faults and where the iron-formation is in contact with the chlorite schist. Layers rich in grunerite weather to a beige color while also exposing the acicular crystal outline. Medium-grained sugary quartz is locally present and stands out on the surface.

Thin section examination reveals the complex textural relationships between these minerals. Generally, the sequence of minerals from oldest to youngest is magnetite, quartz, biotite, almandine, grunerite, stilpnomelane, and chlorite, but this sequence of growth is inconsistent even within the same thin section. Grunerite, magnetite, and quartz are the most abundant minerals observed in thin section (D-5). Both monomineralic layers and medium-grained granules of magnetite are replaced by all the other minerals. Mimetic growth of medium- to fine-grained euhedral magnetite partially preserves banding and crosscuts all the other minerals (NI-7). Granoblastic-polygonal quartz is commonly fine- to medium-grained and overgrows but partially retains the magnetite granule texture. The growth of bladed to fibrous, fine-grained grunerite replaces magnetite layers. Bladed grunerite envelopes golden- to reddish-yellow stilpnomelane and dark olive-green

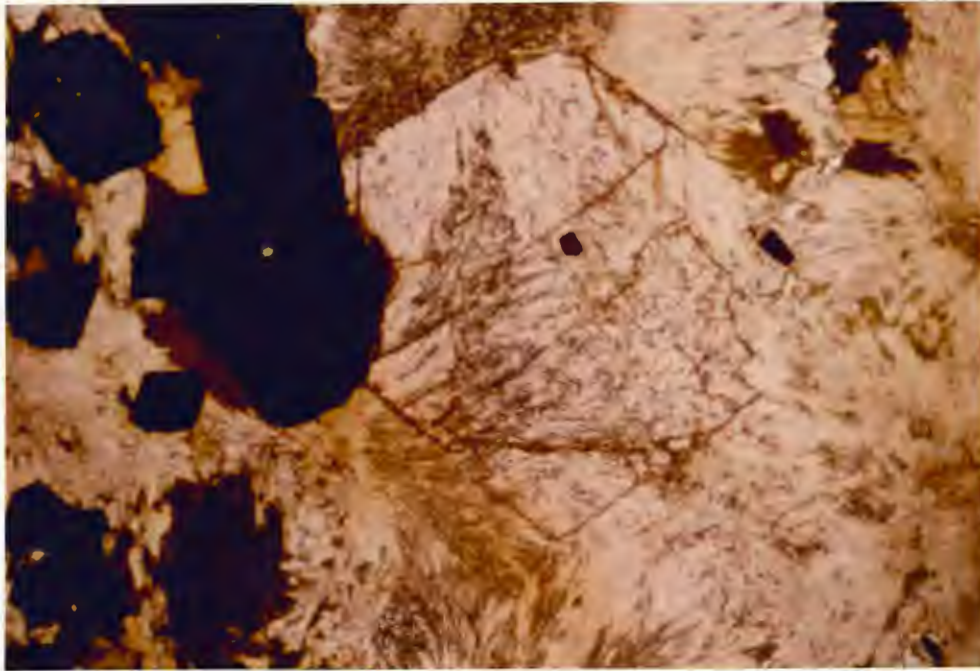


FIGURE 9: Euhedral garnet over fibrous grunerite. Ordinary light. Sample NI-7. Negaunee Iron-Formation. Field of view: 1.8 mm x 2.5 mm.

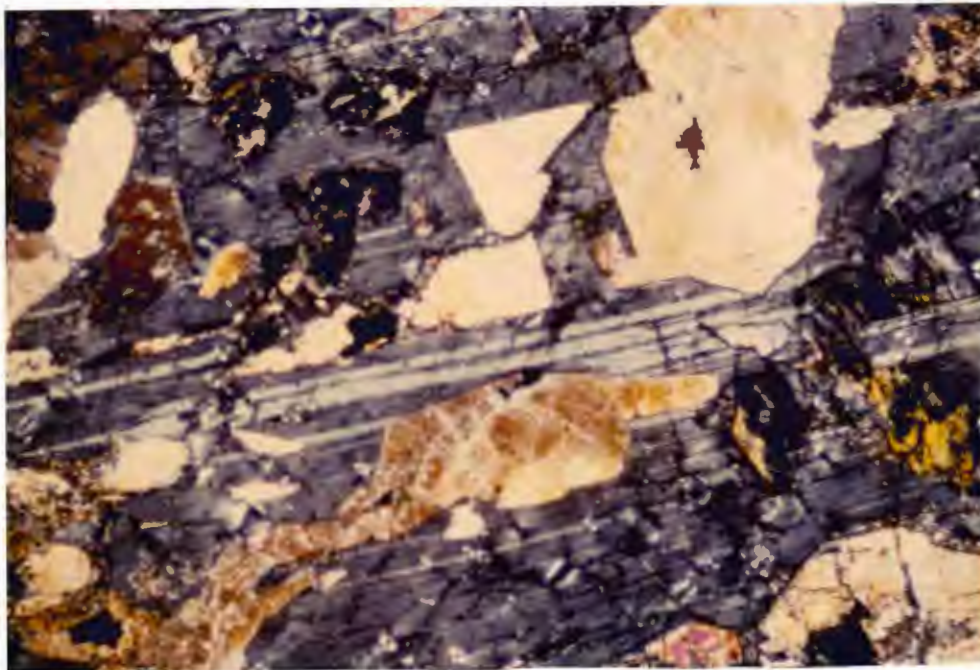


FIGURE 10: Poikilitic intergrowth of plagioclase (twinned, 1st order gray) and augite (2nd order yellow to 3rd order pink). Sample MD-26. Metadiabase, Zone 1. Cross-polars. Field of view: 1.5 mm x 2.3 mm.

biotite but appears to be in equilibrium with chlorite and garnet. Evidence present that platy stilpnomelane is pre-grunerite is given by indistinct inclusions of stilpnomelane within grunerite blades (NI-7). But stilpnomelane crosscuts grunerite in more thin sections (6 versus 4) than those in which it is crosscut by grunerite. Veins of stilpnomelane are found crosscutting all the other minerals where the iron formation is in contact with the chlorite schist (4-37B).

Fine-grained fragments of chlorite and biotite are locally present. Chlorite occurs uncommonly as inclusions in magnetite euhedra, or is interstitial to magnetite granules, or envelopes grunerite (D-5). Biotite may display an interstitial relationship to grunerite, overgrowth by stilpnomelane, and partial alteration to chlorite.

Helicitic dodecahedra of slightly pink garnet overgrow the fibrous grunerite (Figure 9 (NI-7)). Garnet is locally rimmed by stilpnomelane (6-65B, D-5) and fractures are filled with grunerite and biotite. In regions of cataclasis, the garnet porphyroblasts are anhedral, fractured, fine-grained, and concentrated in hematite-rich areas of the rock (6-65B). Garnet dodecahedra are mimetic with respect to and partially replace monomineralic layers of magnetite in the iron-formation where it is in contact with the chlorite schist (4-37A). The dodecahedra are commonly rimmed by chlorite. The mimetic garnet is adjacent to monomineralic layers of garnet which separate the iron-formation from the chlorite schist. Hematite occurs as an oxidation product of both bladed grunerite and subhedral magnetite.

### GOODRICH QUARTZITE

The schist is gray-green and fine-grained. Black chloritoid porphyroblasts, altered off-white chloritoid porphyroblasts, and weathered gold-colored biotite are set in the gray-green matrix of the rock. The schist exhibits a great concentration of chloritoid where it is in contact with the sill and therefore warranted petrographic examination.

The gray-green matrix is predominately sericite and fine-grained chlorite. The chloritoid porphyroblasts reach lengths of 5.1 cm and crosscut the matrix. They exhibit well-defined prismatic boundaries and jagged ends. The chloritoid is either altered partially or totally to chlorite, muscovite, biotite, and medium-grained magnetite. Chlorite and muscovite laths grow along the (001) cleavage plane of the chloritoid. Biotite grows along both parting and cleavage planes of the chloritoid but is replaced by chlorite and magnetite along cleavage planes. Hematite occurs as an oxidation product of magnetite and follows the foliation of the matrix. Euhedral tourmaline is locally present.

### METADIABASE

The metadiabase sill in the Lake Michigamme map area varies mineralogically from a coarse-grained augite- and plagioclase- rich rock at its center to a fine-grained biotite or chlorite-rich schist at its margin. The change from a clinopyroxene-plagioclase rock (diabase) to a schist is gradational and was documented by petrographic examination of 75 thin sections. Certain textures within the least- altered

metadiabase can be traced to the chlorite schist yielding evidence of their common protolith. Striking pseudomorphic features and mineral interactions are seen at the upper margin of the sill in contact with the Negaunee Iron- Formation.

The metadiabase can be divided into four zones on the basis of petrographic character (Plate 1). Zone 1 consists of a plagioclase-clinopyroxene metadiabase. Zone 2 consists of hornblende metadiabase. Relict poikilitic texture is present in both zones. Zone 3 consists of chlorite + hornblende + garnet metadiabase and can be divided into two subzones: In Zone 3A relict poikilitic texture can still be distinguished and there is an increasing amount of chlorite at the expense of hornblende and plagioclase. In Zone 3B, relict poikilitic textures are not discernable. Finally, Zone 4 consists of chlorite or biotite schist + garnet.

#### Zone 1

Zone 1 is found south-east of Coon Lake. It is a narrow zone represented by one sample (MD-26) and is the least altered part of the sill. The rock is a gray to black, medium-grained equigranular diabase. Matte black tabular clinopyroxene grains (5.0 mm long) are intergrown with chalk white feldspar producing a "salt and pepper" appearance on fresh surfaces. Iron staining is seen superficially. The mineral assemblage is plagioclase, augite, magnetite, biotite, hornblende, and minor amounts of apatite, sericite, hematite, and quartz. Table 1 shows the relative proportions of these minerals.

Plagioclase (An <sub>53-57</sub>) laths up to 6mm long poikilitically



TABLE 1: MODAL ANALYSES OF  
SELECTED SAMPLES ACROSS THE METADIABASE (n>300)

| SAMPLE   | AP  | AU   | BI   | CA   | CH   | EP  | GA  | HE  | HO   | MA  | PL   | QU   | SE  | SP  | ZONE |
|----------|-----|------|------|------|------|-----|-----|-----|------|-----|------|------|-----|-----|------|
| MD-26    | 1.9 | 26.9 | 11.3 | -    | -    | -   | -   | -   | 8.4  | 6.5 | 41.4 | 0.2  | 2.4 | -   | 1    |
| MD-25    | 0.2 | -    | 12.3 | -    | 2.7  | 4.3 | -   | tr  | 49.2 | 4.3 | 26.3 | -    | -   | 0.7 | 2    |
| A-3      | 0.5 | -    | 27.7 | -    | 2.0  | 0.7 | -   | -   | 37.0 | 1.5 | 29.7 | 1.0  | -   | -   | 2    |
| 6-256    | 0.2 | -    | 41.6 | -    | 2.9  | 0.7 | -   | -   | 30.7 | 4.9 | 19.0 | -    | -   | -   | 2    |
| 6-238    | -   | -    | 49.9 | 1.2  | 31.1 | -   | -   | -   | -    | 5.1 | 8.8  | 3.9  | -   | -   | 3A   |
| F-4      | 1.4 | -    | 19.0 | tr   | 47.4 | -   | -   | -   | 2.1  | 5.2 | 11.3 | 13.6 | -   | -   | 3A   |
| 23 MD-9  | -   | -    | 24.5 | 7.0  | 4.4  | 0.7 | -   | -   | 20.4 | 1.5 | 31.1 | 10.4 | -   | -   | 3A   |
| NM 10-5  | -   | -    | 34.9 | 1.2  | 34.3 | -   | -   | -   | -    | 5.6 | 11.7 | 12.3 | -   | -   | 3A   |
| A-8*     | tr  | -    | -    | 20.7 | 12.9 | -   | -   | -   | 32.4 | 3.7 | -    | -    | 4.6 | 3.7 | 3A   |
| 4-260    | -   | -    | 16.3 | 2.7  | 39.2 | 2.0 | -   | tr  | 25.8 | 6.3 | -    | 7.8  | -   | -   | 3A   |
| MWD-5    | -   | -    | 24.6 | -    | 41.5 | -   | 4.6 | -   | -    | 9.0 | 18.5 | 1.8  | -   | -   | 3B   |
| 6-204    | -   | -    | 48.4 | 24.3 | 11.0 | -   | 6.3 | 1.2 | 0.2  | 3.7 | -    | 4.9  | -   | -   | 3B   |
| 6-201    | 0.2 | -    | 68.4 | 2.4  | 13.0 | -   | 6.5 | 0.2 | -    | 5.5 | -    | 3.8  | -   | -   | 3B   |
| E-3      | -   | -    | 41.4 | tr   | 44.3 | -   | 1.4 | tr  | -    | 2.6 | -    | 10.3 | -   | -   | 3B   |
| 6-195    | -   | -    | 63.3 | 0.2  | 20.2 | -   | 5.4 | -   | -    | 5.1 | -    | 5.4  | 0.5 | -   | 3B   |
| NM 10-11 | tr  | -    | 58.8 | tr   | 10.2 | -   | 1.0 | -   | -    | 4.3 | 15.7 | 10.0 | tr  | -   | 3B   |

| <u>SAMPLE</u>      | <u>AP</u> | <u>AU</u> | <u>BI</u> | <u>CA</u> | <u>CH</u> | <u>EP</u> | <u>GA</u> | <u>HE</u> | <u>HO</u> | <u>MA</u> | <u>PL</u> | <u>QU</u> | <u>SE</u> | <u>SP</u> | <u>ZONE</u> |
|--------------------|-----------|-----------|-----------|-----------|-----------|-----------|-----------|-----------|-----------|-----------|-----------|-----------|-----------|-----------|-------------|
| NM 10-13           | tr        | -         | 35.2      | -         | 45.9      | -         | 0.3       | tr        | -         | 9.1       | tr        | 9.5       | -         | -         | 3B          |
| MD-14              | -         | -         | 50.4      | -         | 24.6      | 9.6       | -         | -         | 1.4       | 4.0       | 6.0       | 4.0       | -         | -         | 4           |
| D-4                | -         | -         | 46.0      | -         | 33.3      | -         | -         | -         | -         | 5.4       | -         | 15.3      | -         | -         | 4           |
| MD-21 <sup>+</sup> | 0.3       | -         | 46.2      | -         | 25.6      | -         | -         | 1.6       | 0.8       | 7.1       | -         | 9.1       | -         | -         | 4           |
| 6-180-7            | -         | -         | 8.4       | -         | 73.9      | -         | 0.8       | tr        | -         | 13.2      | -         | 3.5       | -         | -         | 4           |
| 6-180-C            | -         | -         | 8.2       | -         | 66.0      | -         | tr        | tr        | -         | 14.7      | -         | 8.6       | -         | -         | 4           |

24

\* Also contains 22.1 % Potassium feldspar

<sup>+</sup> Also contains 9.3 % Grunerite

AP=apatite, AU=augite, BI=biotite, CA=calcite, CH=chlorite, EP=epidote, GA=garnet,  
 HE=hematite, HO=hornblende, MA=magnetite, PL=plagioclase, QU=quartz, SE=sericite,  
 SP=sphene.

enclose augite (Figure 10 (MD-26)). Twin planes are sharp and evidence of strain is minor. Plagioclase has altered to sericite in the cores, and biotite and quartz occur along twin planes, grain boundaries, and random cross-cutting fractures.

Augite grains range in size from 1.6 to 5.0 mm and exhibit simple lamellar twinning. Reaction rims of hornblende are present. Exsolution lamellae of a mineral too fine to identify and biotite occur along cleavage planes in augite.

Hornblende occurs as fine-grained subhedral to anhedral grains with pleochroism ranging from buff ( $\alpha$ ) to olive-green ( $\beta$ ) to blue-green ( $\gamma$ ). The hornblende is locally rimmed by hematite.

## Zone 2

Zone 2 surrounds Zone 1. The rocks in this zone are hornblende metadiabase; all have relict poikilitic texture, but in contrast to the rocks of zone 1, they do not contain augite. They are greenish-black, medium-grained metadiabase. Tabular hornblende grains locally reach 6.0 mm in length and radiate in thick clusters. The poikiloblastic hornblende encloses plagioclase and stands out on the surface due to differential weathering of the chalk-white feldspar, biotite, and quartz. The chalk-white feldspar alters to a soft orange clay on weathered outcrop surfaces. Table 1 shows the changing proportions of minerals from Zone 1 to Zone 2.

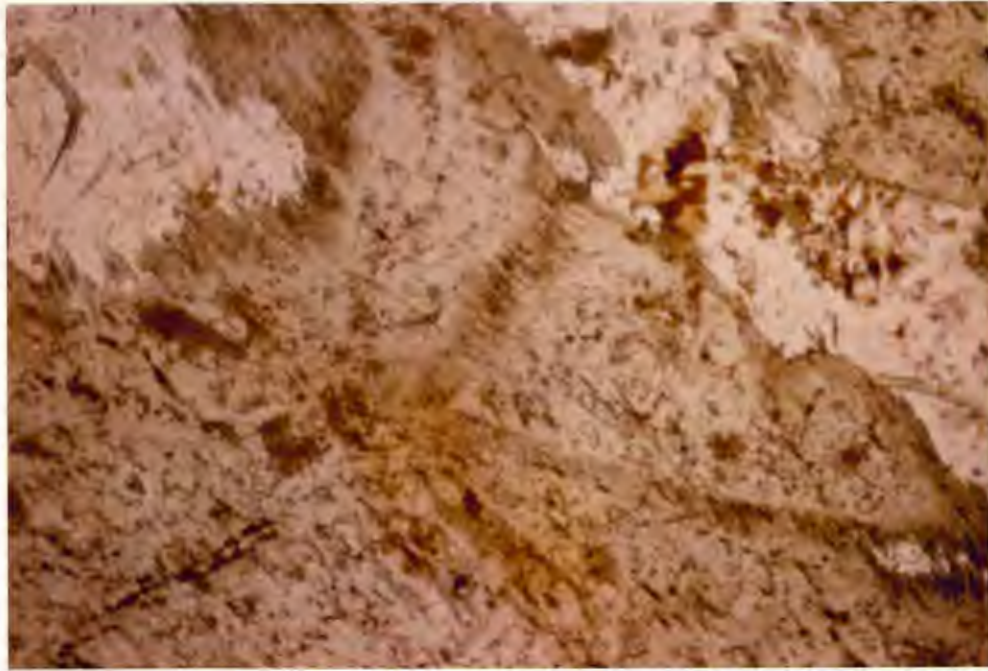
Sample MD-25 (approximately 50 feet north-west of MD-26) shows several textures characteristic of the transition from Zone 1 to Zone 2. Hornblende grains are locally subhedral, larger (3.0 mm to 5.0 mm) and

rimmed by wispy, fine-grained (less than or equal to 0.50 mm in length) hornblende (two periods of hornblende growth are present) or extremely fine-grained aggregates of epidote. The first growth of hornblende will be referred to as hornblende, the second growth of hornblende will be referred to as wispy hornblende. Poikiloblastic hornblende contains plagioclase laths ranging in length from 1.8 to 3.3 mm. Wispy hornblende largely replaces the plagioclase laths which leaves an outline of the plagioclase boundaries in the hornblende (Figure 11 (MD-25)). At other localities epidote occurs as subhedral crystals (0.12 mm in length). Hornblende is altered to medium-grained chlorite and fine-grained calcite along its cleavage planes. Towards the margin of this zone, these two minerals along with predominant quartz (Figure 12 (A-3)) locally pseudomorph hornblende. Apatite also grows preferentially along hornblende's cleavage planes. As alteration proceeds the pleochroic hues of hornblende become faded in patches.

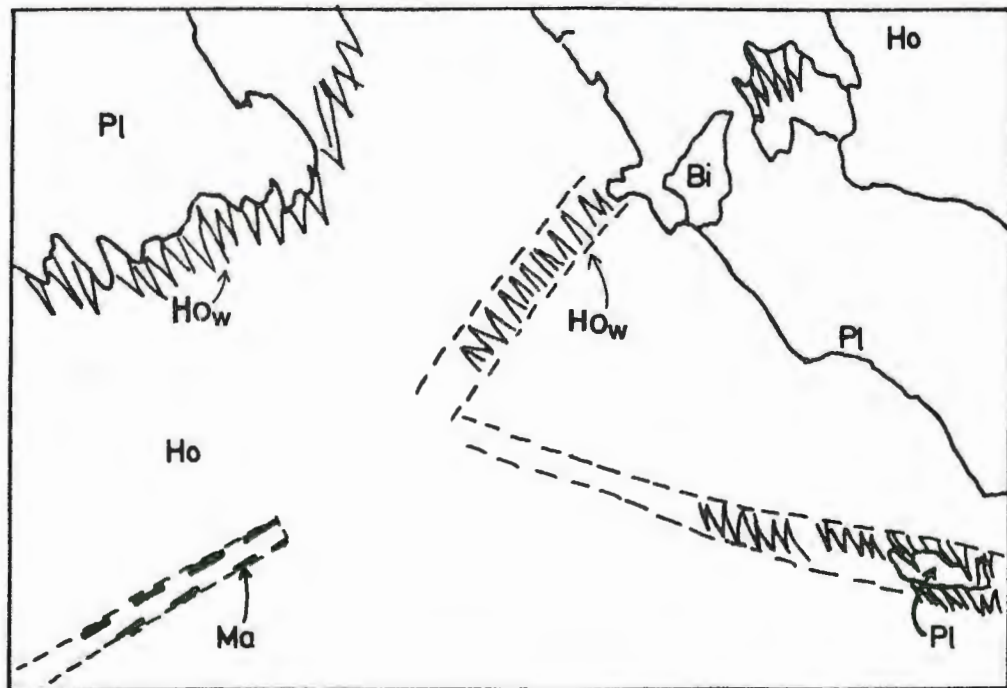
Increased replacement and strain reduces the sharp features of the primary igneous plagioclase; twin planes appear indistinct and subgrain boundaries are present. The replacement is by biotite, chlorite, epidote, calcite, sericite, and acicular hornblende.

Coarse-grained, skeletal, magnetite is included in the hornblende and is rimmed by fine-grained sphene. The sphene-magnetite-secondary hornblende association suggests that sphene may be a by-product of the reaction of augite to hornblende.

Several general trends are observed toward the Zone 2--Zone 3A boundary. The volume percentages of biotite and chlorite increase at



(a)



(b)

FIGURE 11(a): Boundary outline of plagioclase laths preserved within hornblende. Ordinary light. Sample MD-25. Metadiabase, Zone 2. Field of view: 1.75 mm x 2.5 mm.

(b): Sketch of features in (a). Bi=biotite; Ho= hornblende (first growth); Ho =wispy hornblende (second growth); Ma=magnetite/ ilmenite; and Pl=plagioclase.

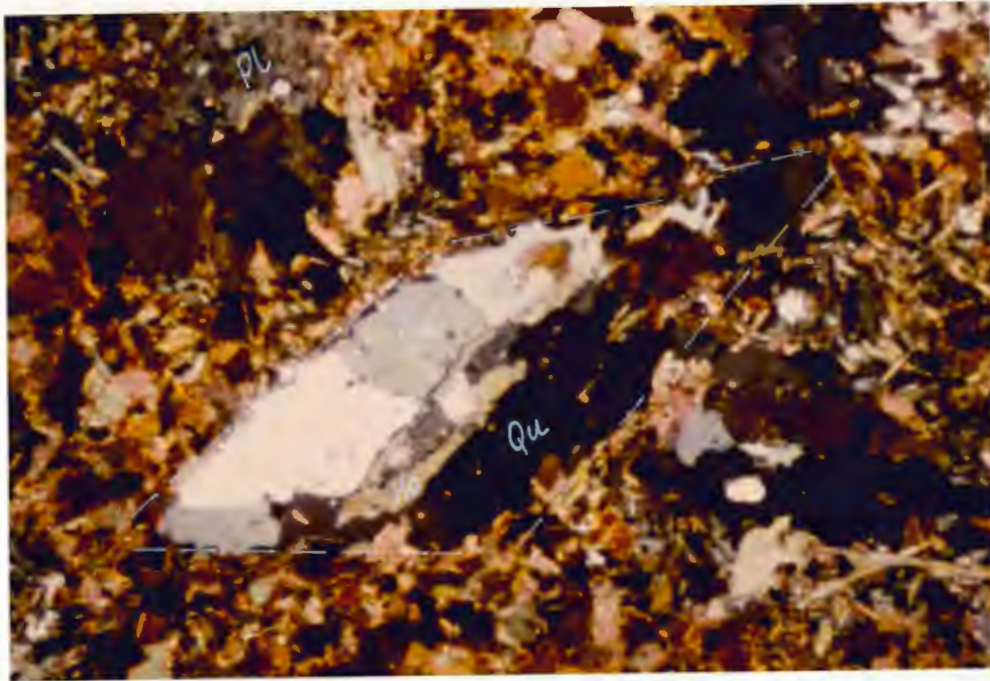


FIGURE 12: Aggregate quartz (white) after hornblende which overgrows plagioclase. Crossed-polars. Sample A-3. Metadiabase, Zone 2. Field of view: 1.5 mm x 2.3 mm.

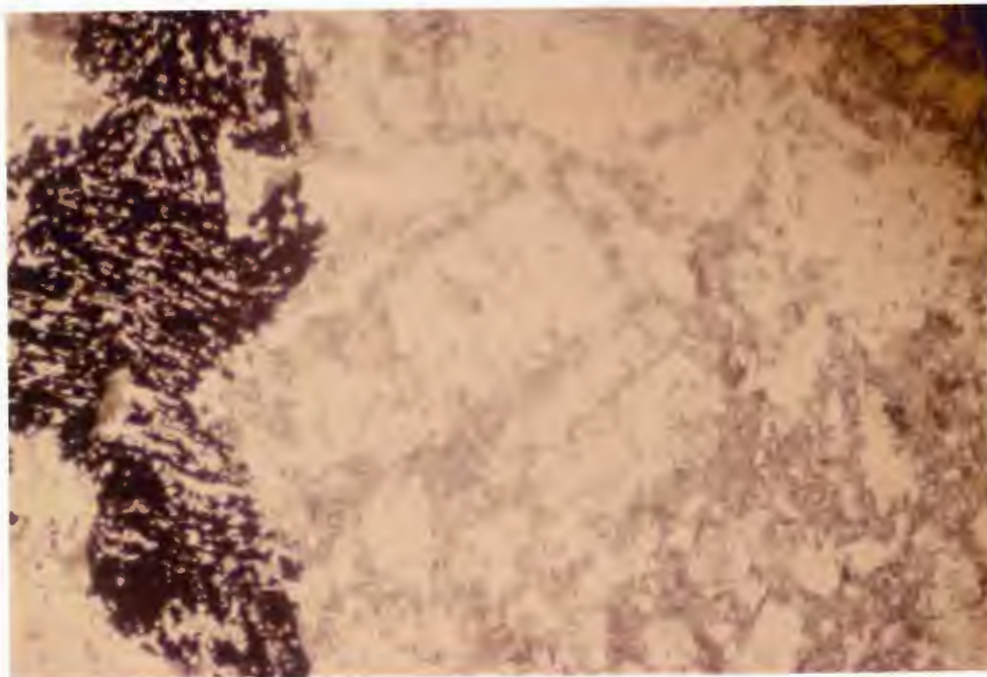


FIGURE 13: Chlorite (gray-green mineral) replacing plagioclase (white) along outer boundaries and twin planes. Ordinary light. Sample F-4. Metadiabase, Zone 3A. Field of view: 1.8 mm x 2.5 mm.

the expense of both plagioclase and hornblende. Biotite, the major alteration product in this zone, and chlorite preferentially replace and divide the plagioclase laths along twin planes reducing them in both dimensions (compare MD-22 (5.0 by 2.0 mm) with 6-256 (3.3 by 0.9 mm) to rectangular or box-like regions (Figure 13 ( F-4)). Wispy hornblende increases in volume. Orthoclase occurs in minor amounts (less than 3 volume percent) and is locally sericitized. It occurs as fine-grained, anhedral grains and is found associated with quartz in cross-cutting veins.

#### Zone 3A

Small areas of relict igneous texture occur in Zone 3A. The rocks vary from dark green to blackish-green, medium-grained metadiabase (locally coarse-grained varieties are seen). Both orthoclase (in cross-cutting veins) and minor plagioclase weather to an orange clay-like material. Although plagioclase and hornblende have random orientation, a slight alignment of the other minerals is observed locally. Poikiloblastic hornblende locally encloses plagioclase. The plagioclase composition may be more sodic ( $An_{37}$ ) than in zone 1 although the determination is from only two samples. Lobate subgrain boundaries, which were restricted to twin planes in previous zones, extend through the entire plagioclase lath. Vermicular intergrowths found in plagioclase suggest that myrmekite is present.

Quartz fills thin fractures in the plagioclase laths, and aggregates of quartz form lenses that are surrounded and partially overgrown by biotite and chlorite. The lenses locally have coarser lobate grains

(less than or equal to 0.9 mm) at their center with undulatory extinction and a rim of finer-grained, partially recrystallized quartz (less than or equal to 0.1 mm)(Figure 14 (F-4)).

At the northern (basal) margin of Zone 3A, biotite is more abundant than chlorite. Hornblende is ubiquitous and alters to calcite, is rimmed by chlorite and quartz, and is associated with hematite (compare to 6-204 which is discussed later). A large size range (0.9 to 3.0 mm) of anhedral hornblende crystals is due to cataclasis. Two episodes of hornblende growth are distinguished by the degree of strain: one is strained and parallel to the slight foliation defined by chlorite; the other is randomly oriented and unstrained (4-260). Plagioclase is seen as optically continuous, anhedral inclusions in hornblende.

Orthoclase is abundant at the contact with the quartzite of the Siamo Slate south of Coon Lake. It occurs as medium-grained laths (1.4 mm long) adjacent to calcite grains but altered to sericite.

Chlorite is the dominant alteration product in the southern part of Zone 3A. Chlorite, with inclusions of sphene, was found to flame into hornblende along its cleavage (Figure 15 (MD-9)). Minor reaction rims of chlorite on hornblende and diamond-shaped sections of chlorite suggest that chlorite pseudomorphed hornblende. Hornblende is locally absent, disappearing in 5.5 meters (18 feet) from Sample 6-256 to Sample 6-238 at the upper margin of the sill.

### Zone 3B

In the field the rocks vary from a dark green to gray-green, fine-grained metadiabase. Locally a slight schistosity is seen due to



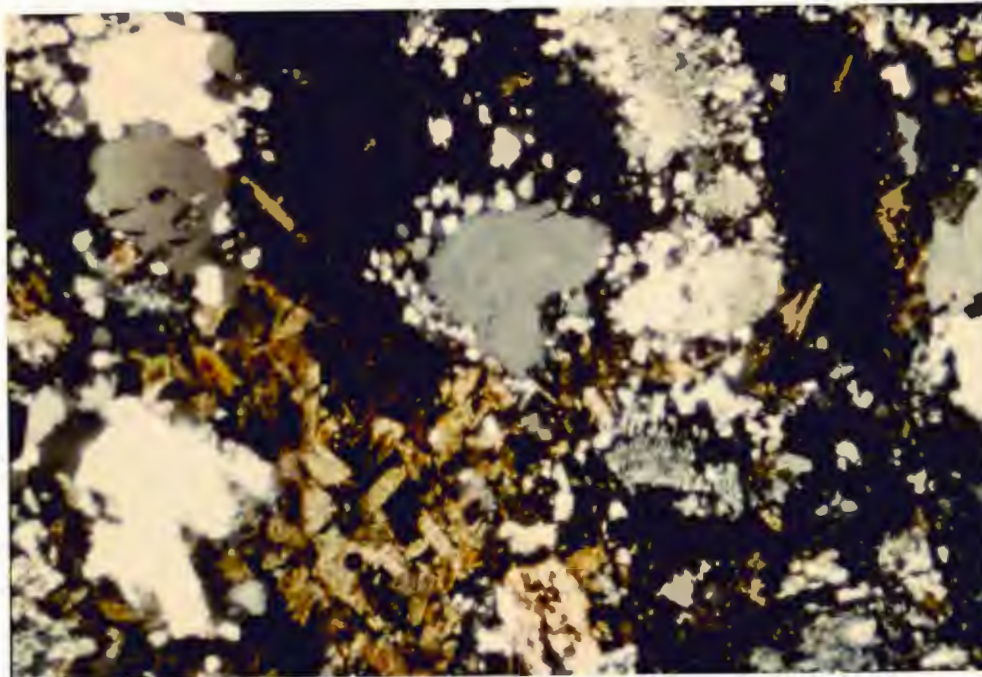


FIGURE 14: Quartz (gray, in center) rimmed by fine-grained quartz (white, gray). Dark areas are chlorite. Crossed-polars. Sample F-4. Metadiabase, Zone 3A. Field of view: 1.8 mm x 2.5 mm.

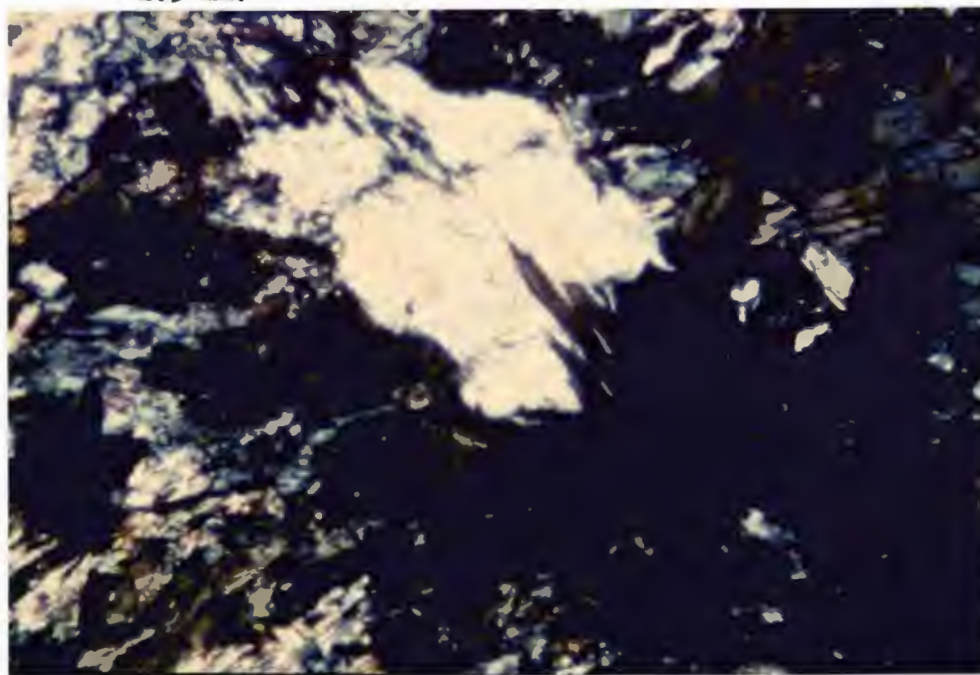


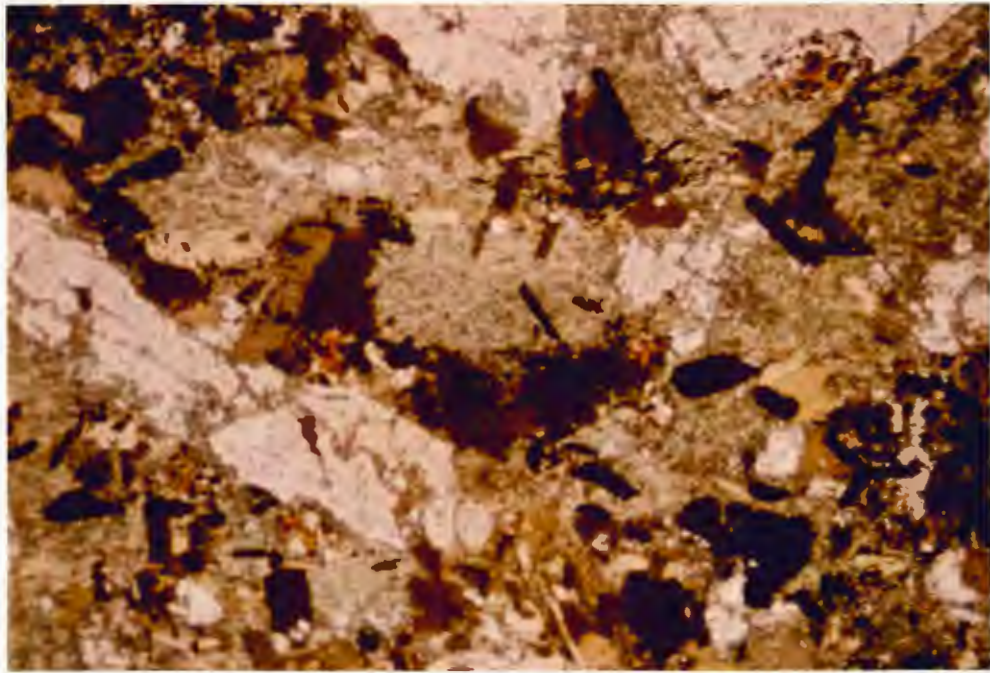
FIGURE 15: Hornblende (2nd order yellow, center) with chlorite (dark) along cleavage, at lower right-hand corner. Sphene inclusions in chlorite are the lighter brown areas. Sample MD-9. Metadiabase, Zone 3A. Crossed-polars. Field of view: 0.4 mm x 0.6 mm.

the abundance of aligned biotite and chlorite. Veins of calcite and orthoclase as well as trace amounts of garnet are present. Several gradational textural changes occur in passing from Zone 3A to Zone 3B. The obliteration of both plagioclase and hornblende comes close to completion resulting in the destruction of the relict poikilitic texture. Garnet appears as subhedral porphyroblasts. Regional tectonic effects are seen in the shearing of chlorite and quartz to lens-shaped regions that are crudely aligned.

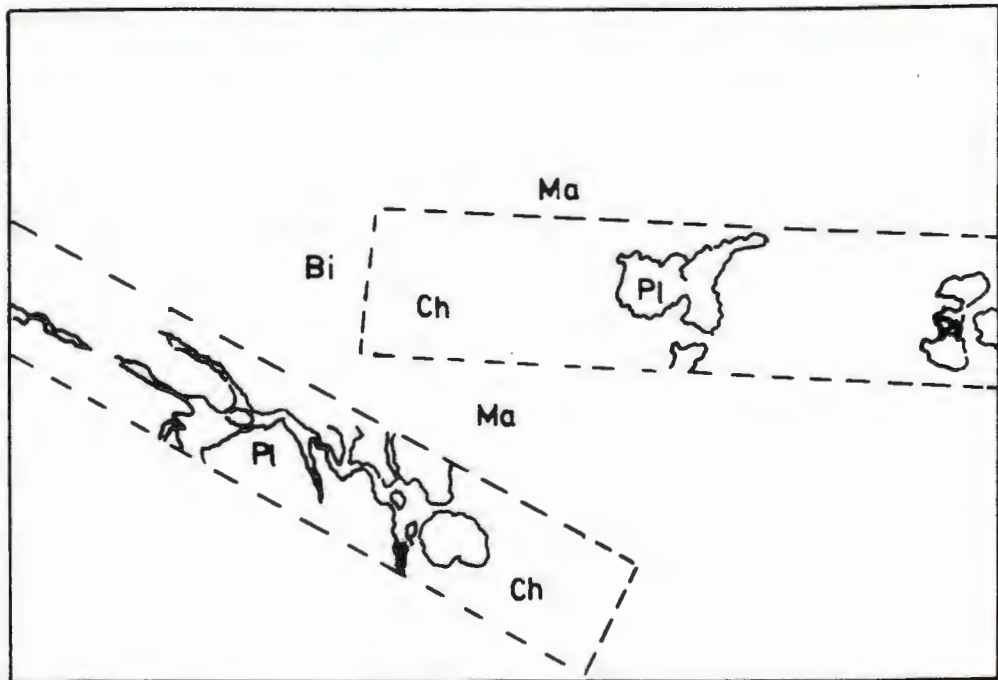
Hornblende partially altered to epidote is abundant near the upper margin of this zone east of Michigamme Mine. Anhedral aggregates of epidote surround an anhedral core of hornblende. Epidote associated with plagioclase is subhedral, fine-grained, and locally zoned.

Drill core taken from Section 19 near the Michigamme Mine documents the changes occurring in the metadiabase (at its southern (upper) margin) as one approaches the metadiabase--iron formation contact. Three thin sections characteristic of Zone 3B were made from core taken from DDH 6: 6-204, 6-201, and 6-195. A sample collected north of the Michigamme Mine dump appears to be slightly out of place but provided valuable insight into the textural changes occurring in this zone (MWD-5). It probably is stratigraphically located between sample 6-204 and sample 6-238 of DDH 6 in Zone 3A.

Although the volume percent of chlorite varies, chlorite along with quartz and biotite are the dominant constituents of the rock. Minor constituents present locally are epidote, sphene, calcite, and sericite. Partial pseudomorphs of chlorite after andesine are present (Figure 16



(a)



(b)

FIGURE 16(a): Chlorite pseudomorph after andesine at center of photomicrograph. Lower left-hand corner--a partially altered plagioclase lath is present. Ordinary light. Sample MWD-5. Metadiabase, Zone 3B. Field of view: 1.75 mm x 2.5 mm.

(b): Sketch of features in (a). Bi=biotite; ch=chlorite; ma=magnetite/ilmenite; pl=plagioclase.

(MWD-5) ). Plagioclase is also replaced by lenses of coarser-grained quartz surrounded by finer-grained quartz.

Porphyroblasts of garnet are fractured and embayed; they are approximately 5.0 mm in diameter but diminish to (0.9mm) closer to the contact. Biotite crudely rims the garnet. Inclusions include quartz (as small aggregates), magnetite, chlorite, and biotite. Alteration along fractures is to muscovite and hematite. Garnet may have grown later than chlorite pseudomorphs after hornblende because it is not chloritized where it is adjacent to them (Figure 17 (6-204)).

Hornblende disappears before plagioclase 7.3 meters (24 feet) north of the metadiabase--iron formation contact in DDH 6 (6-204). Aggregate pseudomorphs of fine-grained hematite and calcite after hornblende are rimmed by chlorite (Figure 18 (6-204)). The diamond-shape pseudomorph of hornblende is distorted to an oval shape. Biotite alters to magnetite and/or ilmenite and they are parallel to the foliation.

#### Zone 4

Zone 4 represents the schistose margins of the metadiabase where it is in contact with the slate to the north and with the iron-formation to the south.

#### Biotite Schist

At the northern limit of the metadiabase the rocks are black, fine-grained, biotite schists. The mineralogy of these schists varies laterally. Ellipsoidal aggregates of fine-grained biotite, epidote, chlorite, and quartz are rimmed by anhedral epidote and aligned with the foliation east of the Baraga--Marquette County line. Distorted

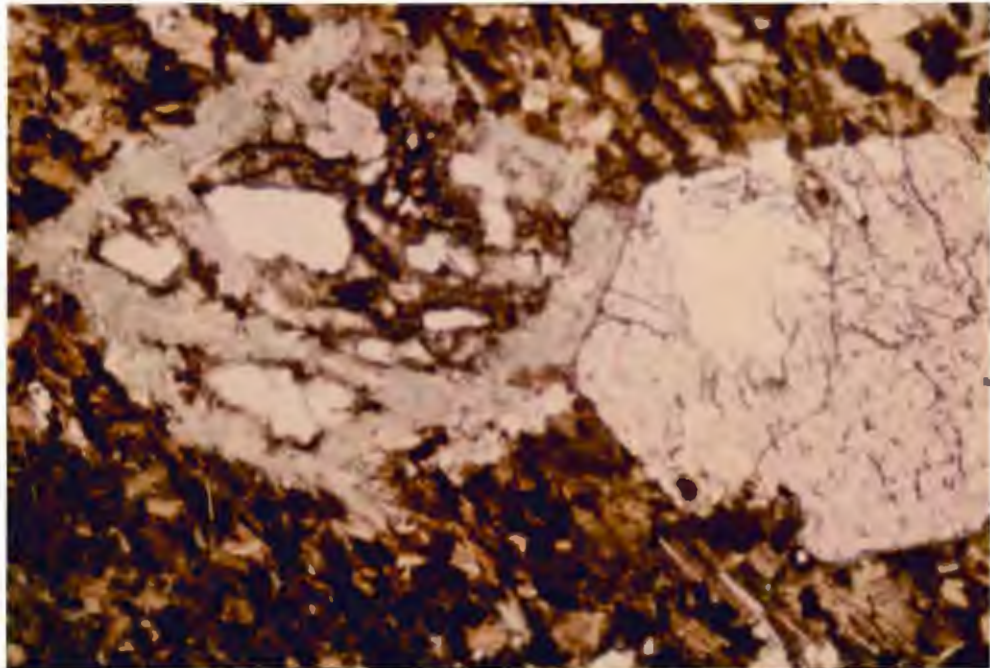


FIGURE 17: Euhedral (6-sided) garnet adjacent to chlorite pseudomorph after hornblende (left side of photomicrograph). Ordinary light. Field of view: 1.8 mm x 2.8 mm. Sample 6-204. Metadiabase, Zone 3B.

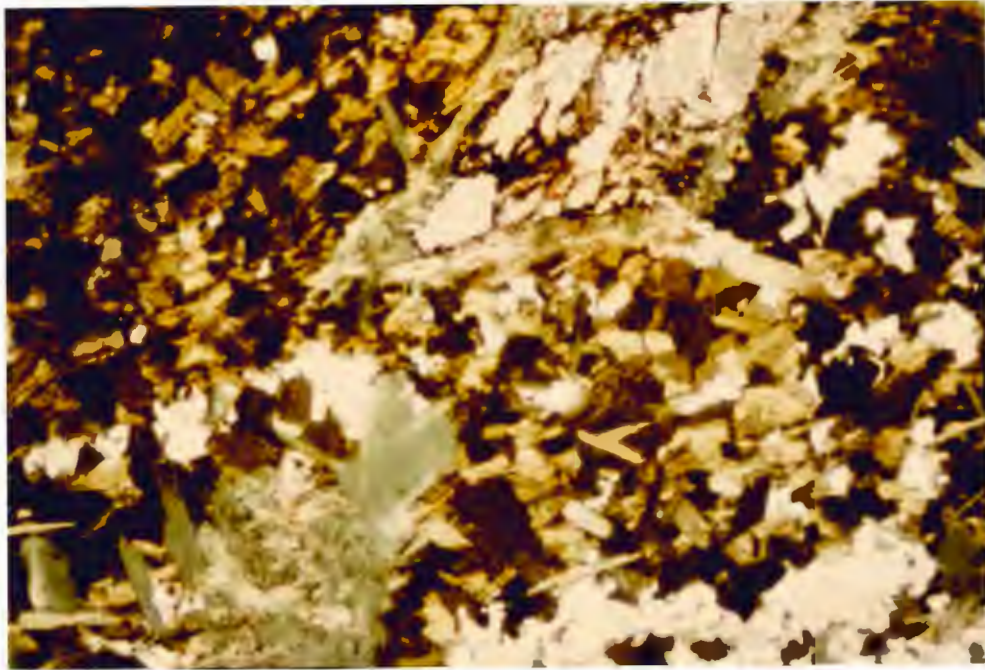


FIGURE 18: Calcite (buff) and hematite (dark) pseudomorph after hornblende rimmed by chlorite (green) (upper right-hand corner). Chlorite pseudomorph after hornblende is in lower left-hand corner. Biotite=olive-brown; quartz=white. Ordinary light. Sample 6-204. Metadiabase, Zone 3B. Field of view: 1.5 mm x 2.3 mm.

tabular regions of aggregate plagioclase are present along with disseminated quartz. Further west, epidote ellipsoids and plagioclase, are absent (D-4, -7, -8, -9). At this location, chlorite, magnetite/ilmenite, biotite, epidote, quartz, and hematite are present.

#### Chlorite Schist

Chlorite schists with a restricted mineral assemblage extend laterally along the contact of the metadiabase and the Negaunee Iron-Formation and occur as thin bodies within the iron-formation. All the schists have  $\geq 40\%$  modal chlorite. Other minerals common to the schists are biotite, magnetite, quartz,  $\pm$  garnet,  $\pm$  grunerite,  $\pm$  apatite,  $\pm$  stilpnomelane,  $\pm$  hematite,  $\pm$  hornblende, and  $\pm$  plagioclase.

The chlorite schist has a unique ellipsoidal texture where aligned ellipsoidal regions (up to 4.0 mm long) of fine-grained chlorite are outlined and defined by a matrix of chlorite, magnetite (and/or ilmenite), and minor biotite and quartz (Figure 19 (6-180-C)). It is well developed and defines the foliation of the rock. Biotite is so fine-grained and scarce that it appears as thin elongated smudges which are parallel to foliation. Tabular-shaped areas of fine-grained chlorite with minor biotite seen in sample MWD-5 resemble pseudomorphs of andesine (Figure 20 (MD-21)). The tabular areas reach dimensions of 6.0 mm by 0.5 mm and locally have a string of biotite laths down their center. The chlorite ellipsoids may have developed from these tabular areas by shearing. Another texture that may link the tabular areas of chlorite with the chlorite ellipsoidal texture is anhedral, aggregate quartz confined to tabular-shaped regions commonly 1.7 mm long.

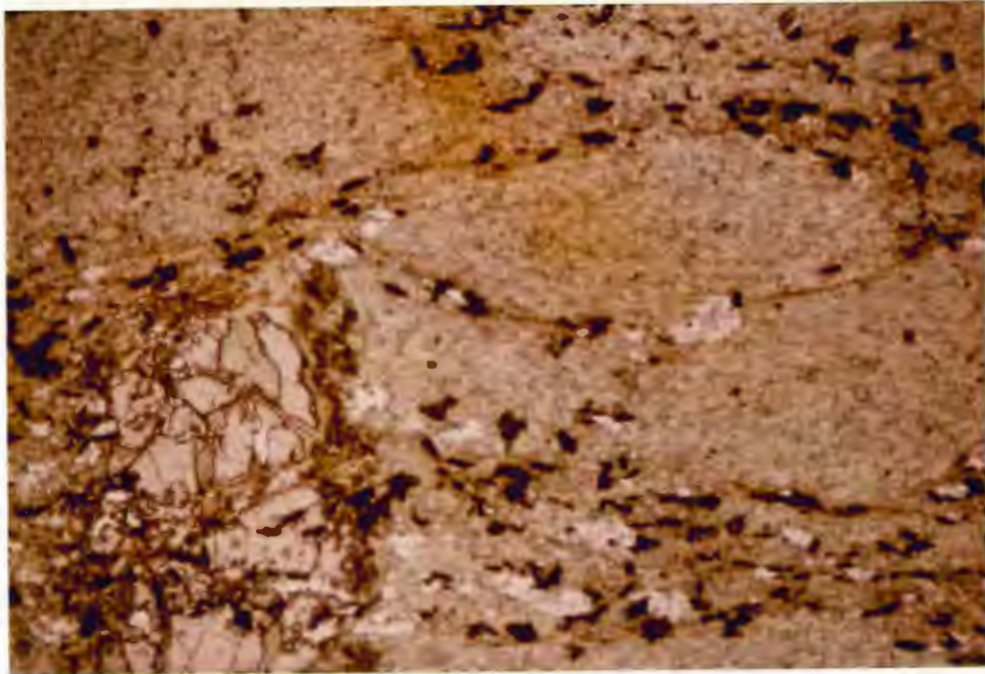


FIGURE 19: Ellipsoid of fine-grained chlorite outlined by magnetite (black), biotite (brown smudges), and quartz (white). Ordinary light. Garnet porphyroblast (lower left-hand corner) overgrows and retains the ellipsoid texture. Sample 6-180-C. Chlorite schist, Zone 4. Field of view: 1.8 mm x 2.5 mm.

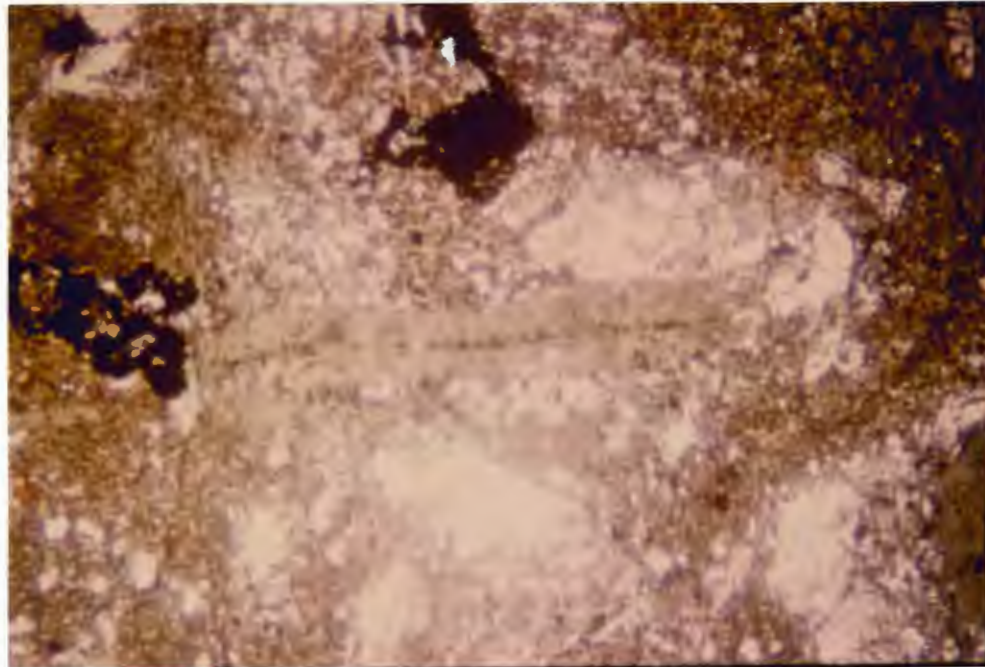


FIGURE 20: Chlorite pseudomorph after plagioclase (center of photomicrograph). Ordinary light. Sample MD-21. Chlorite schist, Zone 4. Field of view: 4.0 mm x 6.0 mm.



Chlorite replaces this quartz texture in the same fashion as it replaces plagioclase feldspar in sample F-4 (compare Figure 13 to Figure 21 (NM-10-13)).

The chlorite schists were sampled from outcrop northwest of the Spurr Mine (MD-21) and from drill hole at two locations adjacent to the Michigamme Mine (DDH 4 and 6). The schists are fine-grained and vary from gray-green, to olive-green, to black. Grunerite blades weather to a tan color and stand out on the surface due to differential weathering of the adjacent minerals northwest of Spurr Mine. Here the mineral assemblage, in order of increasing abundance, is apatite- hornblende- hematite- magnetite- quartz- grunerite- chlorite -biotite. Grunerite crosscuts a matrix consisting of chlorite, biotite, and magnetite and also contains hornblende inclusions. It has a reaction rim of chlorite (oriented normal to the grunerite face with which it reacted) and fine-grained quartz (Figure 22 (MD- 21)). Blades of grunerite, 3.3 mm long, show lamellar twinning and are locally oxidized to hematite.

Grains of anhedral quartz have two sets of fractures oriented at approximately right angles. The quartz boundaries are parallel to these fractures giving a crude diamond shape to the grain. A local foliation of biotite and chlorite wraps around the medium-grained quartz. Biotite laths are partially altered to chlorite along their boundaries. Apatite prisms are 1.0 mm long and are set in the matrix. Skeletal magnetite is coarse-grained and crosscuts chlorite, biotite, and quartz.

Steel-gray needles of grunerite are intergrown with dark red

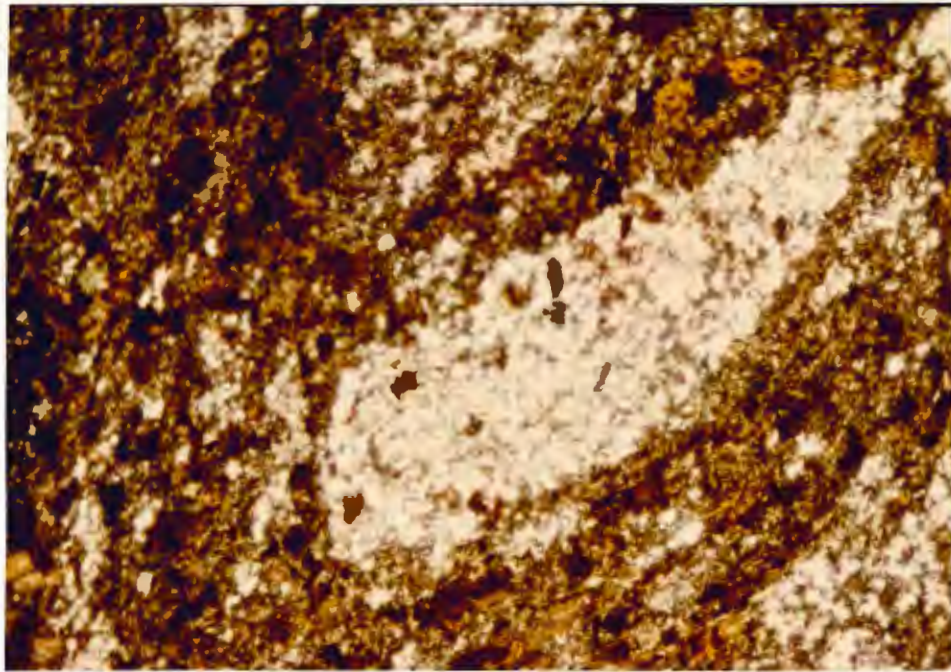


FIGURE 21: Aggregate quartz within distorted tabular area (trends from lower left-hand corner to upper right-hand corner) replaced by chlorite and biotite along boundary of area. Ordinary light. Sample NM 10-13. Metadiabase, Zone 3B. Field of view: 1.5 mm x 3.0 mm.

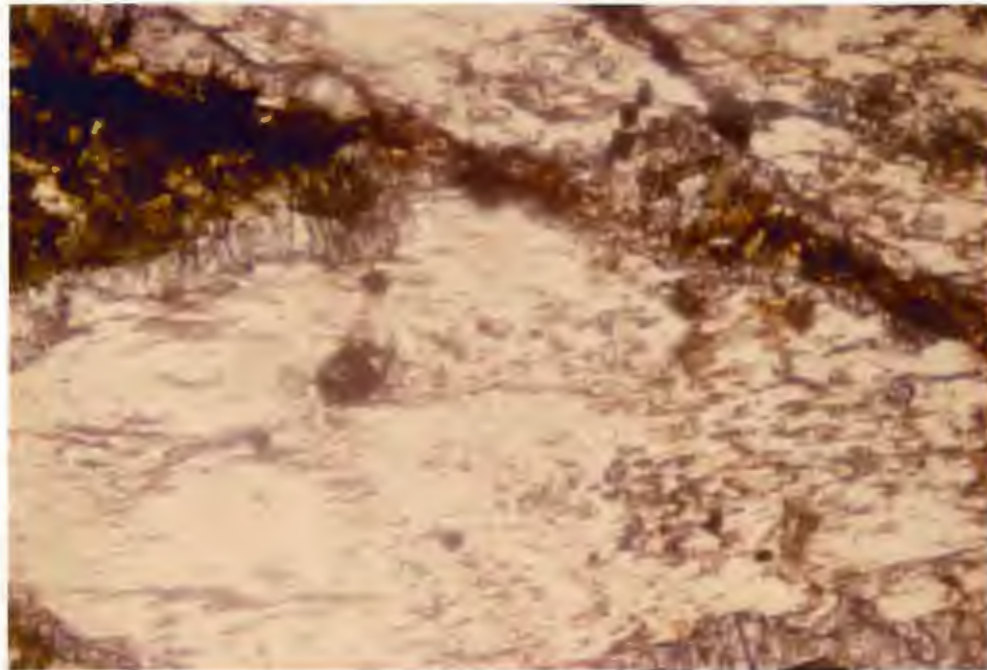


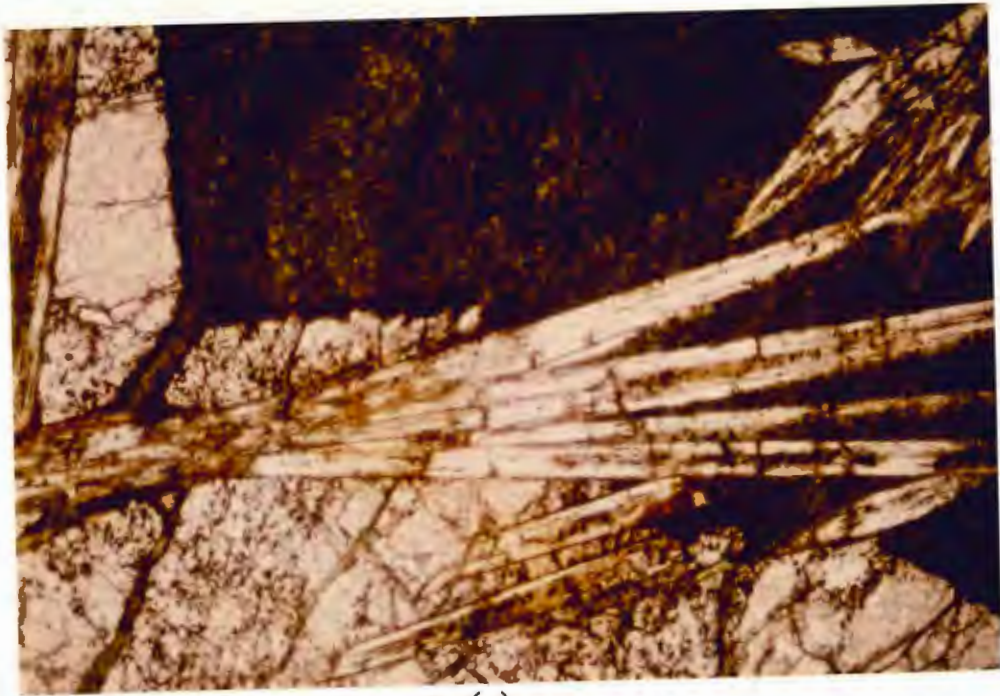
FIGURE 22: Grunerite (large white mineral) rimmed by chlorite and quartz. Ordinary light. Sample MD-21. Chlorite schist, Zone 4. Field of view: 1.8 mm x 2.5 mm.

porphyroblasts of garnet in schists from DDH 4 and 6. The ellipsoidal texture (as outlined by minute grains of magnetite) is continuous through the euhedral to subhedral garnet porphyroblasts (ranging in size from 0.9 to 3.0 mm), grunerite blades, and chlorite-filled fractures of the garnet (Figure 23 (4-15)). Grunerite also penetrates the chlorite ellipsoids. The textural relationship between garnet and grunerite is complex. The thin stilpnomelane rim around garnet either is pierced by grunerite blades or crosscuts them. Stilpnomelane is distinguished from biotite by having a higher birefringence and lacking birds eye maple extinction. When stilpnomelane is absent, biotite occurs as inclusions in garnet or diffuse brown smudges in the matrix (4-15) or anhedral broken grains replaced by magnetite and associated with chlorite. Green stilpnomelane also is found as an aggregate pseudomorph replacing tabular sections of carbonate (MWD-4). This pseudomorph in turn is partially overgrown by chlorite.

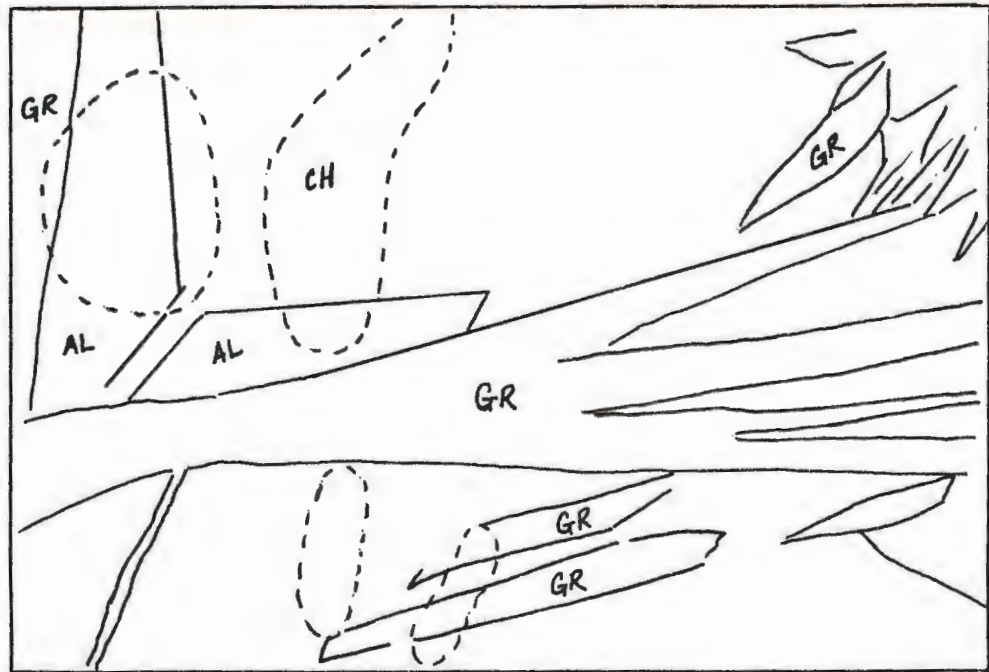
Fine-grained quartz occurs as either anhedral grains disseminated in the matrix, aggregates confined to tabular-shaped regions, or inclusions in garnet.

#### Chlorite Schist-Negaunee Iron-Formation Contact

The contact between the chlorite schist and the iron-formation is interfingering despite the size of the sill and this interfingering is observed in drill core (Figure 8). An assemblage of almandine-chlorite- magnetite- pyrite- quartz- stilpnomelane is found in both lithologies in very different proportions except that the assemblage of the schist does not contain pyrite. The chlorite schist is



(a)



(b)

FIGURE 23: a. Chlorite ellipsoids, outlined by magnetite (black), trend parallel to width of photomicrograph. The ellipsoidal texture is continuous through garnet (white), grunerite (white bladed mineral), and chlorite-filled fractures in the garnet. Ordinary light. Sample 4-15. Metadiabase (chlorite schist), Zone 4. Field of view: 1.5 mm x 2.3 mm.

b. Sketch of (a).

distinguished from the iron-formation by the following criteria: iron-formation is typically brecciated and contains dominantly quartz and magnetite; the chlorite schist consists dominantly of chlorite with chlorite ellipsoids present. Primary textures in the iron-formation such as oolites and granules (both 0.9 mm diameter) are truncated by quartz veins (Figure 24 (4-37A2)). Euhedral pyrite (up to 2.0 mm diameter) is found in the iron-formation. Garnet dodecahedra (0.5 to 2.0 mm diameter) and magnetite octahedra (0.5 mm) grew mimetically within magnetite or chlorite schist layers. The dodecahedra of garnet grade into monomineralic layers of helicitic garnet that commonly separates the iron-formation and the chlorite schist. The chlorite ellipsoidal texture is preserved in the garnet layer whose width varies from a few millimeters (at locale depicted in Figure 8 ) to several centimeters (Figure 25 (NM 11-7)). The chlorite schist also contains cross-cutting veins of stilpnomelane.

#### Summary

A relict poikilitic texture of labradorite and augite located in Zone 1 can be correlated to a relict poikilitic texture of plagioclase and hornblende which is present through Zone 3A of the sill. The chlorite schist contains an ellipsoidal texture which can be traced from Zone 3B of the metadiabase. This texture is present in the schist regardless of whether it is a small body in the iron-formation or found between the iron-formation and the sill. The texture developed prior to the growth of almandine and grunerite. The Negaunee Iron-Formation is separated from the chlorite schist by almandine and is commonly

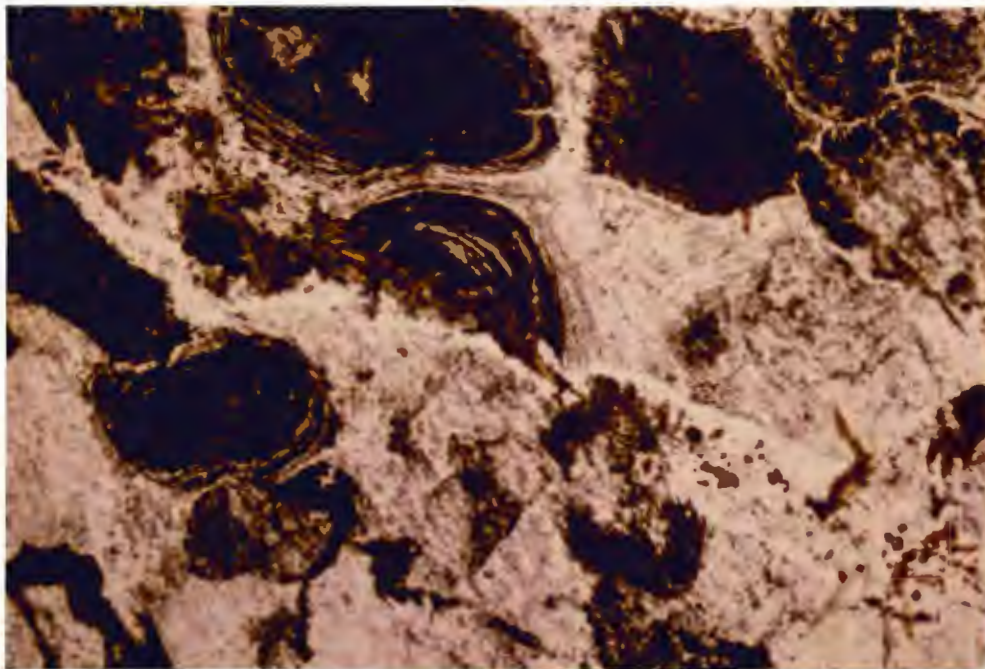


FIGURE 24: Brecciated iron-formation. Quartz vein oriented diagonally across photomicrograph. Note truncated granules and grunerite crosscutting quartz vein. Ordinary light. Sample 4-37A2. Field of view: 1.8 mm x 2.8 mm.

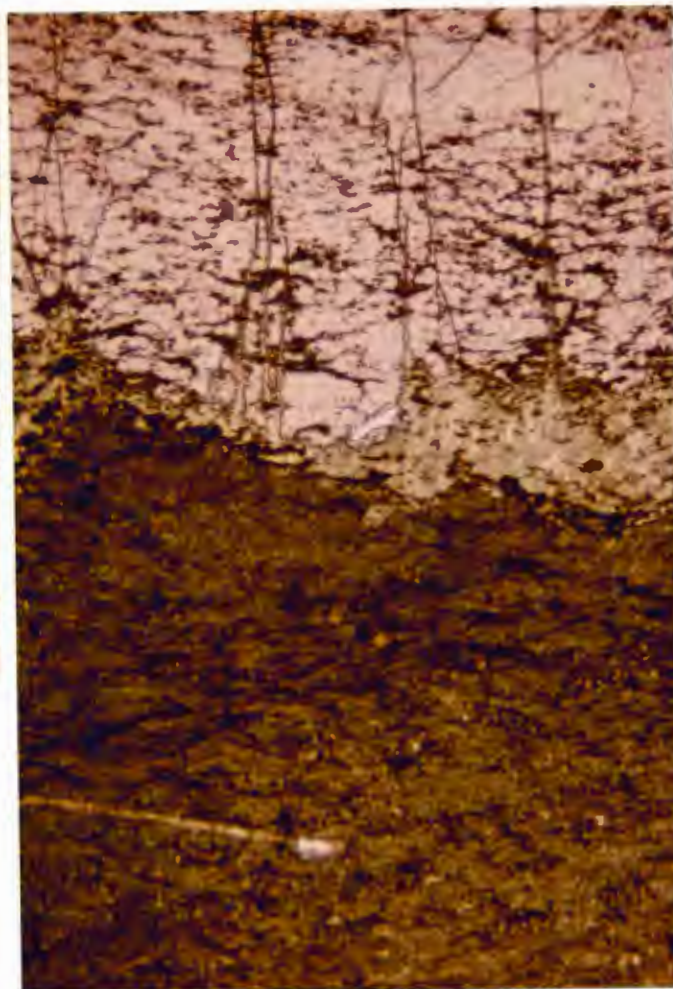


FIGURE 25: Almandine layer (top of photomicrograph) separating iron-formation from chlorite schist (bottom of photomicrograph). Retrograde chlorite is juxtaposed between almandine and chlorite schist. Ordinary light. Sample NM 11-7. Field of view: 4.0 mm x 6.0 mm.

brecciated.

## CHEMICAL ANALYSIS

Whole rock chemical analysis was carried out on a suite of eleven samples from several locations across the metadiabase sill to examine the changes in major element chemistry across the sill toward the contact with the Negaunee Iron- Formation. The samples document the change from the relatively unaltered metadiabase to the highly- altered metadiabase (chlorite schist) at the upper margin of the sill. The samples were analyzed at Michigan Technological University in Houghton, Michigan on a Phillips automated X-ray spectrometer (AXS). Analysis, calibration, and data reduction were accomplished by accompanying interactive software. Further information on the XRF at MTU can be obtained in Rose et al (1985). The results are given in Tables 2A and 3. The major elements are tabulated in weight percent of the oxides while the trace elements are recorded as weight percent of the elements or parts per million (ppm). <sup>\*</sup> FeO in Table 2 represents total iron.

Major oxide abundances observed across strike from the least altered metadiabase (MD-26) to the chlorite schist (6-180-C) change as follows:

- 1)  $\text{SiO}_2$ ,  $\text{CaO}$ ,  $\text{Na}_2\text{O}$  all decrease.
- 2)  $\text{TiO}_2$  vacillates, decreases slightly.
- 3)  $\text{Al}_2\text{O}_3$  increases slightly.
- <sup>\*</sup>
- 4)  $\text{FeO}$  increases significantly.
- 5)  $\text{MnO}$  increases.
- 6)  $\text{MgO}$  increases.
- 7)  $\text{K}_2\text{O}$  initially increases but then decreases below its



TABLE 2: A: COMPOSITION (IN WT %) OF SELECTED SAMPLES ACROSS THE METADIABASE  
TOWARD ITS UPPER MARGIN

| Zone:  | 1                              | 3A           | 3A             | 3B           | 3B           | 3B           | 3B         | 3B              | 3B              | 4              | 4              |       |
|--------|--------------------------------|--------------|----------------|--------------|--------------|--------------|------------|-----------------|-----------------|----------------|----------------|-------|
|        | <u>MD-26</u>                   | <u>6-238</u> | <u>NM 10-5</u> | <u>MWD-5</u> | <u>6-204</u> | <u>6-201</u> | <u>E-3</u> | <u>NM 10-11</u> | <u>NM 10-13</u> | <u>6-180-7</u> | <u>6-180-C</u> |       |
| 47     | SiO <sub>2</sub>               | 47.89        | 41.74          | 49.13        | 41.60        | 40.00        | 36.75      | 37.59           | 44.32           | 37.57          | 33.19          | 34.60 |
|        | TiO <sub>2</sub>               | 3.66         | 2.25           | 2.64         | 3.40         | 2.73         | 2.06       | 3.16            | 2.33            | 2.87           | 3.04           | 2.74  |
|        | Al <sub>2</sub> O <sub>3</sub> | 11.42        | 11.60          | 12.57        | 12.57        | 10.76        | 10.11      | 12.48           | 13.60           | 12.30          | 12.49          | 12.03 |
|        | FeO*                           | 16.87        | 22.79          | 17.64        | 25.30        | 27.53        | 26.19      | 28.53           | 20.53           | 29.44          | 39.88          | 39.68 |
|        | MnO                            | 0.21         | 0.74           | 0.21         | 0.77         | 1.20         | 0.92       | 0.34            | 0.24            | 0.32           | 0.61           | 0.79  |
|        | MgO                            | 2.22         | 6.75           | 4.30         | 3.34         | 4.47         | 5.26       | 5.49            | 4.16            | 6.14           | 5.49           | 5.21  |
|        | CaO                            | 8.07         | 1.32           | 1.58         | 0.96         | 1.76         | 2.44       | 0.50            | 1.12            | 0.58           | 0.20           | 0.13  |
|        | Na <sub>2</sub> O              | 2.02         | <0.2           | 1.11         | 1.57         | <0.2         | <0.2       | <0.2            | 0.93            | <0.2           | <0.2           | <0.2  |
|        | K <sub>2</sub> O               | 1.28         | 4.69           | 3.60         | 2.14         | 5.37         | 6.39       | 3.91            | 6.04            | 2.61           | 0.68           | 0.03  |
|        | P <sub>2</sub> O <sub>5</sub>  | 0.73         | 0.21           | 0.28         | 0.34         | 0.22         | 0.25       | 0.24            | 0.23            | 0.20           | 0.05           | 0.01  |
|        | BaO                            | 0.14         | 0.14           | 0.11         | 0.13         | 0.11         | 0.09       | 0.14            | 0.14            | 0.11           | 0.09           | 0.07  |
| Total: | 94.51                          | 92.43        | 93.17          | 92.12        | 94.15        | 90.47        | 92.38      | 93.64           | 92.14           | 95.72          | 95.29          |       |

TABLE 2. NATURAL VERSUS EXPERIMENTAL METABASALTS PRODUCED BY REACTION OF SEA WATER WITH BASALT AT HIGH WATER ROCK RATIOS (wt %; ppm for trace elements)

|                                | *Metabasalts: 23.6° N.<br>Mid-Atlantic Ridge<br>All96: |        |       |        | †Experiments: 300°C.<br>Basalt glass + Sea-water<br>Sea-water: rock ratio: |       |       |
|--------------------------------|--|--------|-------|--------|--|-------|-------|
|                                | 15-1   | 15-3   | 15-13 | 14-15  | 50   | 62    | 125   |
| SiO <sub>2</sub>               | 49.11  | 42.45  | 49.39 | 46.95  | 44.90  | 43.74 | 38.99 |
| TiO <sub>2</sub>               | 0.49   | 2.19   | 0.85  | 1.46   | 1.92   | 1.63  | 2.17  |
| Al <sub>2</sub> O <sub>3</sub> | 16.72  | 16.98  | 16.03 | 16.58  | 14.13  | 15.09 | 16.66 |
| FeO*                           | 9.71   | 15.74  | 8.30  | 11.73  | 14.20  | 12.17 | 10.78 |
| MnO                            | 0.17   | 0.19   | 0.17  | 0.05   | 0.08   | 0.05  | 0.03  |
| MgO                            | 10.96  | 11.73  | 15.42 | 15.13  | 15.96  | 17.50 | 19.69 |
| CaO                            | 6.09   | 3.18   | 0.29  | 0.27   | 0.14   | 0.88  | 0.17  |
| Na <sub>2</sub> O              | 2.57   | 0.80   | 1.34  | 0.11   | 0.10   | 0.08  | 0.03  |
| K <sub>2</sub> O               | 0.05   | 0.01   | 0.01  | 0.05   | 0.06   | 0.10  | 0.11  |
| P <sub>2</sub> O <sub>5</sub>  | 0.09   | 0.52   | 0.07  | 0.29   | 0.28   | 0.22  | 0.16  |
| CO <sub>2</sub>                | 0.10   | 0.17   | 0.03  | 0.07   |  |       |       |
| H <sub>2</sub> O*              | 4.18   | 7.09   | 7.46  | 8.47   | 7.55   | 7.96  | 11.01 |
| Σ                              | 100.24   | 101.05 | 99.36 | 101.16 | 99.32  | 99.42 | 99.80 |
| FeO                            | 6.82   | 11.84  | 6.80  | 10.26  | 8.17   | 6.89  | 8.83  |
| Fe <sub>2</sub> O <sub>3</sub> | 3.69   | 5.69   | 2.42  | 1.63   | 6.71   | 5.86  | 2.17  |
| Rb                             | 0.4  |        | 2.2   | 0.5    |  |       |       |
| Sr                             | 129  | 109    | 12    | <5     |  |       |       |
| Ba                             | <20  | <20    | <20   | <20    | 10   | 4     | <1    |
| V                              | 182  | 320    | 179   | 233    | 435  | 432   | 447   |
| Cr                             | 189  | 203    | 344   | 180    | 151  | 146   | 152   |
| Co                             | 52   | 60     | 38    | 78     | 35   | 58    | 32    |
| Ni                             | 106  | 117    | 132   | 88     | 93   | 116   | 92    |
| Cu                             | 9  | 5      | 64    | 5      | 3  |       | 12    |
| Zn                             | 66   | 64     | 91    | 26     | 44   | 58    | 43    |
| Y                              | 17   | 53     | 20    | 37     |  |       |       |
| Zr                             | 42   | 173    | 50    | 121    |  |       |       |
| Nb                             | 1.0  | 6.3    |       | 2.7    |  |       |       |

\*Analysis by X-ray fluorescence spectrometry.

†Analysis by DC-plasma emission spectrometry; anhydrite was removed by dissolution prior to analysis; from Seyfried and Mottl (1982).

TABLE 2: B: Table 2 from Mottl (1983) p. 166. Compare to Table 2-A. 14-15 is the most-altered metabasalt.

TABLE I

Metagabbros from dredge A150-RD20

| Specimen No.                   |        | AM11  | AM30  | AM33    | AM7   |
|--------------------------------|--------|-------|-------|---------|-------|
| FeO*/MgO                       | weight | 0.52  | 0.86  | 1.62    | 2.28  |
| Fe/(Mg + Fe)                   | atomic | 0.23  | 0.33  | 0.48    | 0.56  |
| SiO <sub>2</sub>               |        | 48.58 | 47.74 | 43.04   | 25.40 |
| TiO <sub>2</sub>               |        | 0.61  | 0.59  | 3.46    | 0.89  |
| Al <sub>2</sub> O <sub>3</sub> |        | 10.17 | 15.19 | 15.36   | 18.91 |
| Fe <sub>2</sub> O <sub>3</sub> |        | 1.64  | 1.53  | 3.17    | 0.97  |
| FeO                            |        | 5.79  | 7.71  | 11.64   | 28.78 |
| MnO                            |        | 0.13  | 0.15  | 0.23    | 0.28  |
| MgO                            |        | 14.04 | 10.61 | 8.93    | 13.00 |
| CaO                            |        | 12.32 | 10.03 | 9.00    | 0.00  |
| Na <sub>2</sub> O              |        | 2.91  | 2.63  | 2.66    | 0.03  |
| K <sub>2</sub> O               |        | 0.07  | 0.08  | 0.11    | 0.01  |
| H <sub>2</sub> O <sup>-</sup>  |        | 1.03  | 0.19  | 0.45    | 0.11  |
| H <sub>2</sub> O <sup>+</sup>  |        | 2.59  | 2.89  | 2.03    | 11.39 |
| P <sub>2</sub> O <sub>5</sub>  |        | 0.00  | 0.02  | 0.02    | 0.01  |
| Cr <sub>2</sub> O <sub>3</sub> |        | —     | —     | 0.006   | 0.02  |
| NiO                            |        | —     | —     | 0.013   | 0.09  |
|                                | Total  | 99.88 | 99.36 | 100.119 | 99.39 |
| FeO*                           |        | 7.27  | 9.09  | 14.49   | 29.65 |
| (CIPW norm)                    |        |       |       |         |       |
| or                             |        | 0.41  | 0.47  | 0.65    | 0.1   |
| ab                             |        | 19.26 | 22.25 | 20.01   | 0.3   |
| an                             |        | 14.48 | 29.41 | 29.65   | —     |
| ol                             |        | 13.70 | 16.58 | 24.80   | 51.0  |
| hy                             |        | —     | 7.89  | —       | 15.1  |
| di                             |        | 37.16 | 16.34 | 12.21   | —     |
| mt                             |        | 2.17  | 2.17  | 2.17    | 1.4   |
| il                             |        | 1.16  | 1.12  | 6.57    | 1.7   |
| ap                             |        | 0.00  | 0.05  | 0.05    | —     |
| cm                             |        | —     | —     | 0.01    | —     |
| ne                             |        | 2.91  | —     | 1.35    | —     |
| c                              |        | —     | —     | —       | 18.9  |
|                                | Total  | 59.19 | 44.15 | 45.81   | 69.2  |

The first three columns show relatively weakly chloritized metagabbros, while the last column an almost completely chloritized one (i.e., a chlorite rock). FeO\* means total iron as FeO. The norms in the first three columns were calculated after partial reduction of Fe<sub>2</sub>O<sub>3</sub> to 1.5%.

TABLE 2: C: Table 1 from Miyashiro (1979) p. M47. Compare to Table 2 A and 2B.

TABLE 3: TRACE ELEMENTS (IN PPM) FOR SELECTED SAMPLES  
ACROSS METADIABASE TOWARD UPPER MARGIN OF SILL

| Zone: | 1            | 3A           | 3A             | 3B           | 3B           | 3B           | 3B         | 3B              | 3B              | 4              | 4              |
|-------|--------------|--------------|----------------|--------------|--------------|--------------|------------|-----------------|-----------------|----------------|----------------|
|       | <u>MD-26</u> | <u>6-238</u> | <u>NM 10-5</u> | <u>MWD-5</u> | <u>6-204</u> | <u>6-201</u> | <u>E-3</u> | <u>NM 10-11</u> | <u>NM 10-13</u> | <u>6-180-7</u> | <u>6-180-C</u> |
| Rb    | 33           | 107          | 76             | 36           | 80           | 105          | 68         | 117             | 56              | 12             | 3              |
| 50 Sr | 152          | 22           | 319            | 118          | 27           | 22           | 20         | 225             | 24              | -              | -              |
| V     | 370          | 255          | 303            | 441          | 324          | 241          | 397        | 278             | 365             | 390            | 381            |
| Cr    | 73           | 363          | 287            | 127          | 170          | 2485         | 341        | 591             | 296             | 580            | 590            |
| Ni    | 34           | 47           | 29             | 25           | 38           | 117          | 33         | 29              | 27              | 10             | 2              |
| Cu    | 427          | -            | 47             | 34           | 67           | 37           | 14         | 68              | 281             | 11             | 5              |
| Zn    | 114          | 60           | 89             | 85           | 66           | 141          | 119        | 93              | 114             | 94             | 88             |
| Y     | 63           | 22           | 22             | 21           | 23           | 23           | 21         | 27              | 15              | 10             | 15             |
| Zr    | 237          | 80           | 120            | 113          | 56           | 48           | 82         | 85              | 85              | 70             | 65             |
| Nb    | 20           | 17           | 12             | 18           | 16           | 14           | 15         | 12              | 16              | 13             | 14             |
| La    | 51           | 14           | 17             | 45           | 27           | 21           | 37         | 19              | 30              | 31             | 17             |
| Ce    | 325          | 196          | 214            | 299          | 213          | 152          | 288        | 206             | 237             | 229            | 176            |

initial value.

- 8)  $P_2O_5$  decreases slightly.
- 9) BaO decreases slightly.

The major element chemistry is compatible with the petrography observed in the sill.  $SiO_2$ , CaO, and  $Na_2O$  all decrease in concentration towards the upper margin of the sill.  $Ca^{2+}$  loss is observed first in Zone 2. The leached  $Ca^{2+}$  reacts with the fluid in the other zones of the sill where minor veins of calcite (6-204) are found and pseudomorphs after hornblende are observed (Zone 2). The increased loss of  $Ca^{2+}$  and  $Na^+$  at the margins of the sill is correlated with the absence of plagioclase and hornblende there. A decrease in  $SiO_2$  is substantiated at the upper margin of the sill by the abundance of chlorite -- a low silica mineral. But large milky quartz veins and layers are present in fractures at the upper margin of the sill and they indicate that the freed  $SiO_2$  precipitated in these fractures. Potassium decreases in concentration toward the upper margin of the sill.

Figure 26 shows a plot of whole rock analyses of three rare-earth elements normalized to chondrites (average chondrite values taken from Haskin et al, 1968) versus rare-earth atomic number. A similar pattern is found for each sample across the metadiabase. The similarity of these patterns is evidence that the protolith of the chlorite schist was diabase. These samples are also compared to the Mesabi iron-formation (Fryer, 1977) which is similar to the Negaunee Iron-Formation in composition and age. Rare-earth elements in iron-formations show a low concentration in these elements (Fryer, 1977) and a different pattern

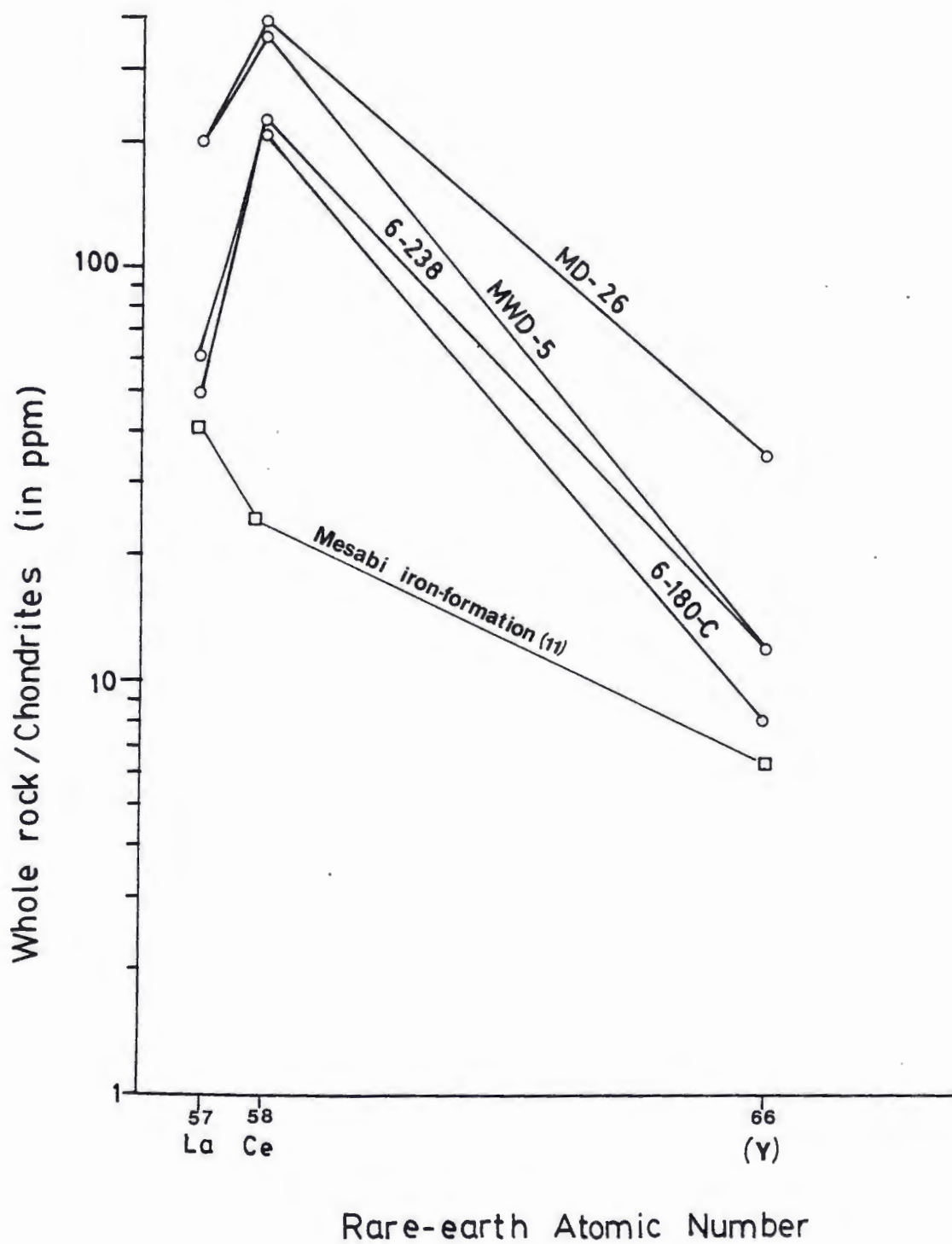


FIGURE 26: Rare- earth elements normalized to chondrites versus atomic number. MD-26: least-altered metadiabase; 6-180-C: most-altered metadiabase (chlorite schist).

from the sill.

Concentration versus distance was used in plotting the minor elements across the zones in the metadiabase. This method was used to examine the mobility of these elements during hydrothermal alteration.

Nb, Sc, Zr, Zn, V remained fairly constant across this contact suggesting immobile behavior (Figure 27). Cu, Ni, Rb, Sr exhibit erratic behavior in the metadiabase and decreased significantly in the chlorite schist suggesting mobile behavior during alteration (see Figures 27 and 28). Rb and Sr are chemically similar to K and Ca respectively and therefore should behave similarly during alteration. They decrease in concentration towards the contact.

#### COMPARISON WITH MODERN HYDROTHERMAL SYSTEMS

Miyashiro et al. (1979) studied a suite of metagabbros taken from the bottom of the Atlantis fracture zone across the Mid-Atlantic Ridge (MAR) at 31° N at a depth of 4140 meters. Mottl (1983) examined a suite of metabasalts taken from 23.6° N along the MAR and dredged from fault scarps along the axial valley of the MAR. They note the following changes in major oxide abundance as the chloritized rock is approached from the relatively unaltered basalt (see Table 2B and 2C).

- 1)  $\text{SiO}_2$ ,  $\text{CaO}$ ,  $\text{Na}_2\text{O}$  decrease.
- 2)  $\text{TiO}_2$  vacillates and increases.
- 3)  $\text{Al}_2\text{O}_3$  increases (Mottl's decreases slightly, essentially constant).
- 4)  $\text{FeO}$  increases significantly.
- 5)  $\text{MnO}$  increases slightly (Mottl's decreases).

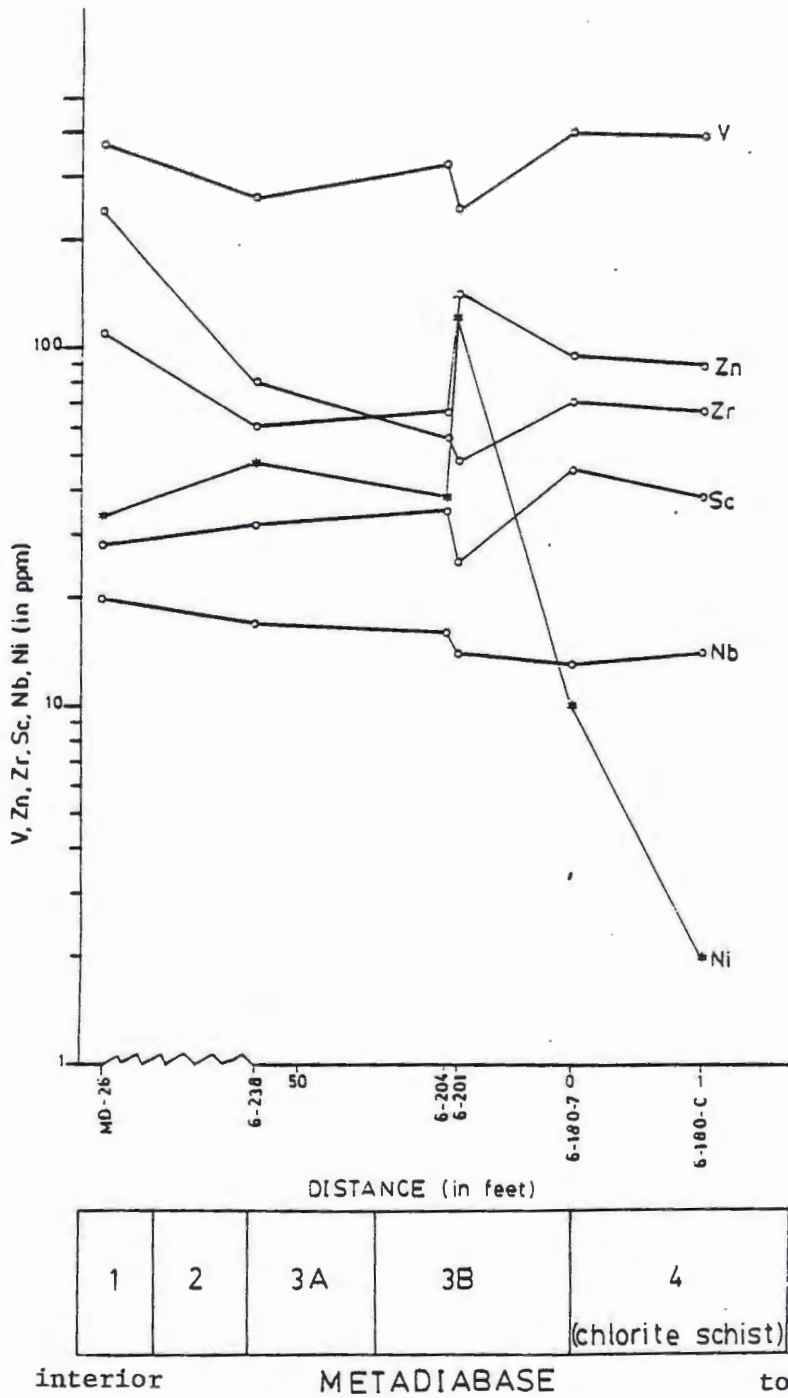


FIGURE 27: Trace element concentration versus distance across the sill towards its upper margin.



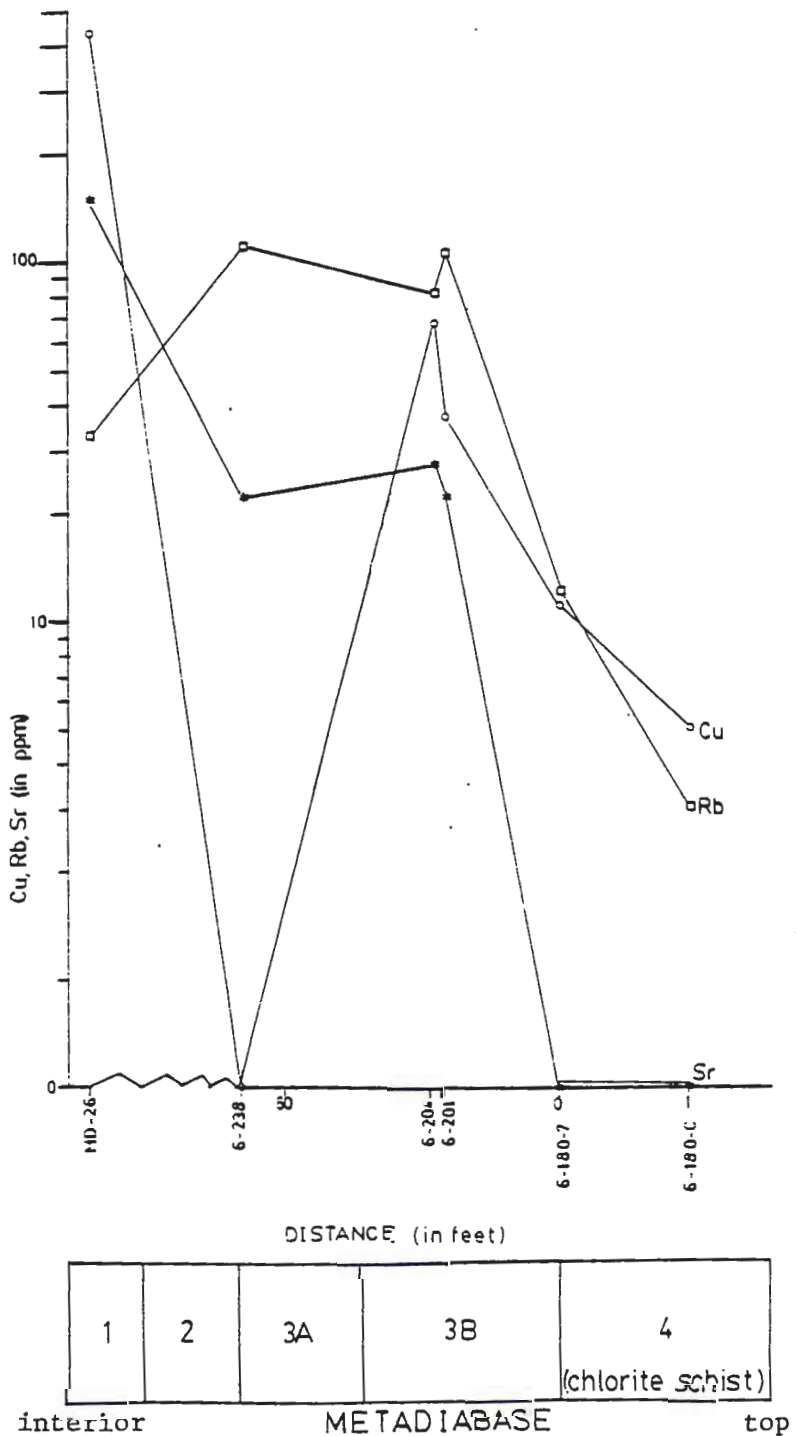


FIGURE 28: Trace element concentration versus distance across the sill towards its upper margin.

- 6) MgO decreases (Mottl's increases).
- 7)  $K_2O$  decreases (erratic behavior--Mottl).
- 8)  $P_2O_5$  increases.

These patterns are similar to those from the metadiabase suite taken from the Lake Michigamme area with the exception of  $TiO_2$ ,  $MgO$  (Miyashiro),  $MnO$  (Mottl), and  $P_2O_5$ . All three suites show iron enrichment toward the most-altered sample (1.2 times greater in the Mottl suite, 2.5 times greater in the Michigamme suite, and 4 times greater in the Miyashiro suite).

Mottl (1983) compares the natural metabasalts with experimentally-produced metabasalts. The experimental basalts were subjected to varying sea-water-to-rock ratios at a temperature of  $300^\circ C$  (Table 2-B). A higher seawater-to-rock ratio is indicative of a more-altered basalt. The major element changes observed in the experimental basalts towards the higher fluid to rock ratios correspond to the changes observed in the natural basalts except that  $Al_2O_3$  increases and  $FeO$  decreases. The experiments show that a major chemical exchange occurs between Mg from the seawater and Ca from the basalt (Mottl, 1983). The resulting effect on the altered rock would be a loss of Ca toward the reacting interface and likewise an increase in Mg towards this same interface. Similar trends are observed in the metadiabase suite from the Lake Michigamme area while only a Ca-loss is observed in the Miyashiro suite.

Mottl noticed a positive correlation between the behavior of Fe and Mg in the natural metabasalts. The growth of chlorite was dependent on

how much fluid interacted with the rock because chlorite growth was correlated with the amount of Mg present. Chlorite-rich rocks show Fe-enrichment which may be due to local redistribution of the element to sites of chlorite formation (Mottl, 1983) since they did not show enrichment in the experimental basalts. Iron-enrichment in the Miyashiro and Lake Michigamme suites indicates that more than local redistribution occurred in order to produce such a great concentration of iron. The Negaunee Iron-Formation could provide an abundant source of iron for the Lake Michigamme sill.

A model predicting the mineral assemblages one would expect to find with varying seawater to rock ratios is given in Figure 29 (Mottl, 1983). The least-altered metadiabase (Zone 1) shows little evidence of hydrothermal alteration and its assemblages cannot be applied to Figure 29 (see also Figure 30). Zone 2 and 3A samples commonly bear quartz, plagioclase, amphibole, epidote, chlorite (and uncommonly sphene) (Table 1). Mottl's model yields fluid/rock ratios of less than 30 for the analogous assemblages. Samples from Zones 3B and 4 uncommonly bear plagioclase or amphibole or epidote and commonly contain quartz and chlorite (Figure 30). This suggests fluid/rock ratios of more than 50. This suggests that the upper margin of the sill was altered under a strongly fluid-dominated system, the rest of the sill being altered under a much less fluid-dominated system. The development of chlorite occurred sporadically at the upper margin of the sill (it is absent south of Michigamme Methodist Institute). The distribution of fractures in the Negaunee Iron-Formation probably controlled which areas of the

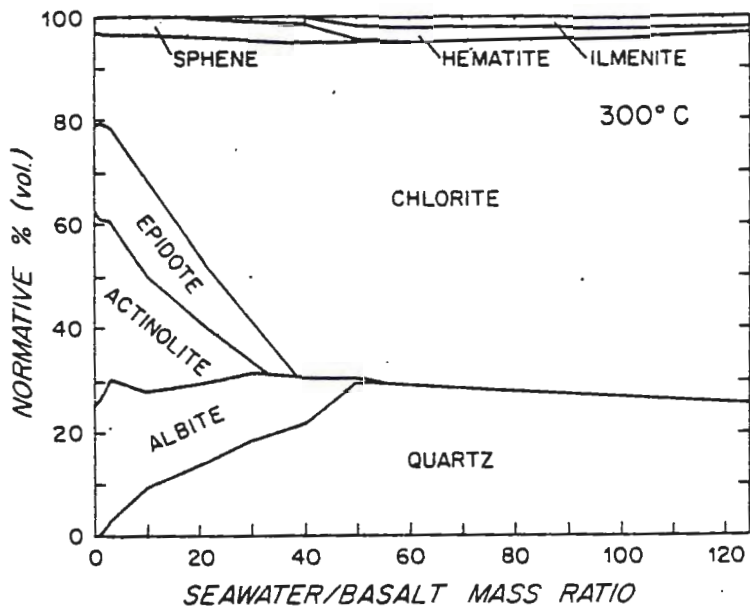


FIGURE 29: Model predicting the mineral assemblages and proportions that are produced when basalt reacts with varying amounts of sea water within the greenschist facies. The model is based on chemical data from basalt--sea water experiments at 300°C and 500 to 600 bars (Mottl, 1983, Figure 4).

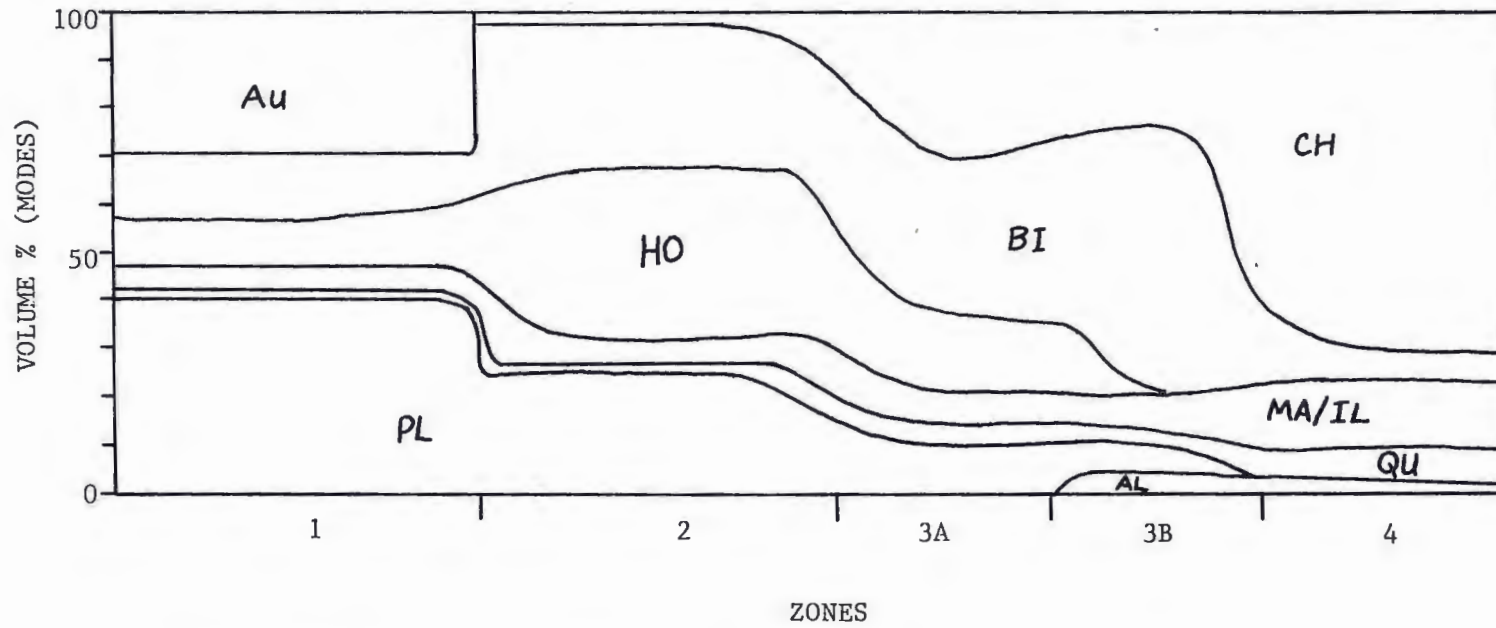


FIGURE 30: Visual representation of mineral assemblages and proportions across the zones of the sill. Mineral abbreviations given in Table 1.

upper margin of the sill received and reacted with the most fluid.

Mottl (1983) also examined trace element behavior with increase in alteration in both the natural and experimental basalts. The behavior of Ba, Sr, V, Ni, and Zn is similar in these and in the Lake Michigan suite.

#### SUMMARY

The behavior of the major elements across the sill is comparable to the behavior of major elements in several modern seawater alteration suites such as those of Miyashiro and Mottl.  $\text{FeO}^*$  and  $\text{MgO}$  increase while  $\text{SiO}_2$ ,  $\text{CaO}$ , and  $\text{Na}_2\text{O}$  all decrease in abundance. The comparison is good, although the environment of the sill differs in many respects from the MAR, and the similar major element patterns may be due to the sill being adjacent to a banded iron-formation. Rare-earth element data and other relatively immobile trace elements verifies a common protolith for the chlorite schist and the metadiabase sill. The mineral assemblage in the chlorite schist indicates alteration occurred in a strongly - fluid dominated system. The minor elements are mobile as expected in a fluid-dominated hydrothermal system.

## INTERPRETATION

In this section, the question to be addressed is essentially whether major hydrothermal alteration predated or accompanied regional metamorphism. This will be accomplished by examining the major mineral assemblages and their relation to the bulk composition in the sill. Mineral assemblages and the interpreted reactions in the iron-formation will also be discussed. Finally, the most-altered metadiabase will be related to the iron-formation by examining assemblages present in both lithologies.

These assemblages should indicate if alteration predated or accompanied regional metamorphism. If alteration predated regional metamorphism the assemblages would be compositionally dependent whereas reaction with fluids might explain their distribution if alteration accompanied regional metamorphism. Textures found in the sill suggest that major hydrothermal alteration predated regional metamorphism because almandine and grunerite crosscut hydrothermally-derived chlorite which recrystallized when the schist was formed. Equilibrium assemblages (as inferred from textures) are compatible with regional metamorphism which suggests that hydrothermal alteration did not postdate regional metamorphism.

The distribution of minerals in equilibrium and the relations between these minerals are affected by the metasomatic changes in the sill which occurred due to the hydrothermal event and can be shown on a CFM diagram (Abbott, 1982). The CFM diagram is valuable because it links the three lithologies: metadiabase, chlorite schist, and iron-

formation. The apexes are:  $C = \text{CaO} - \text{Al}_2\text{O}_3 + \text{Na}_2\text{O} + \text{K}_2\text{O}$ ;  $F = \text{FeO}$  (where total iron is given as FeO, which differs from Abbott's definition of  $F = \text{FeO} - \text{Fe}_2\text{O}_3$ ); and  $M = \text{MgO}$ .

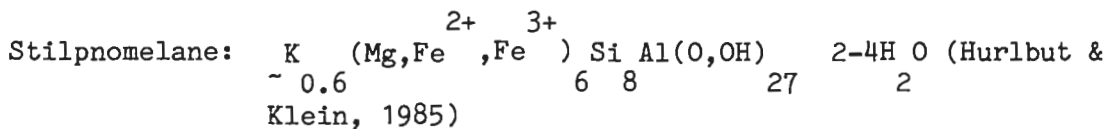
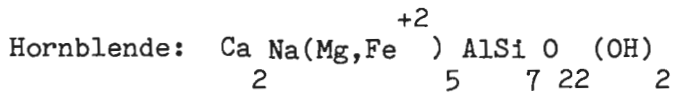
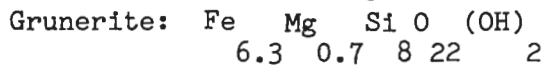
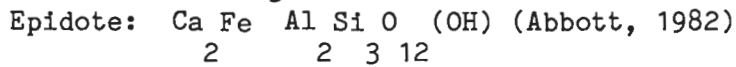
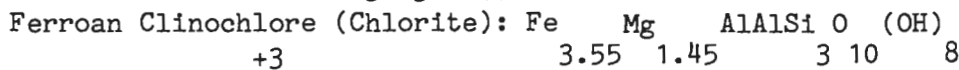
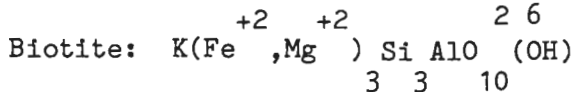
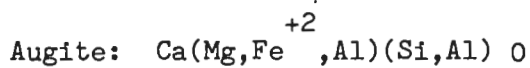
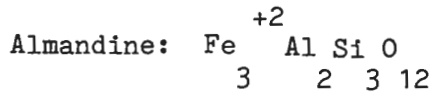
Table 4 lists the formulas used to determine the position of the minerals on the CFM diagram (Figure 31). The order of  $X = F/(F + M)$  for several of the minerals was taken from Abbott (1982) and Veblen and Ribbe (1982). Table 5 lists the possible equilibrium assemblages observed in each zone of the sill and in the iron-formation. The CFM diagram for the study area was plotted by combining the above data to show the dominant relations that occurred in the various lithologies (Figure 32). Quartz, plagioclase, potassium feldspar, magnetite, and water vapor may be part of each assemblage because the CFM diagram is projected from them (Abbott, 1982).

Modal analysis of the metadiabase shows the major mineral changes across the metadiabase (Table 1, also see Figure 30). In Zone 1, augite, plagioclase, biotite, and hornblende are the abundant minerals. In Zone 2, augite disappears and a major assemblage of biotite, chlorite, hornblende, plagioclase, and quartz is present. This is also the dominant assemblage found in Zone 3A although hornblende is absent at some locations (6-238, NM 10-5). In Zone 3B, plagioclase and hornblende disappear while almandine appears resulting in an assemblage of almandine, biotite, chlorite, and quartz.

These changes are compatible with the mineral relations shown on the CFM diagram (see Figure 32). An assemblage of au- bi- ho in Zone 1 disappears as the bulk composition of the sill changes. It is replaced



TABLE 4: ASSUMED FORMULAS OF MINERALS IN THE METADIABASE  
AND NEGAUNEE IRON- FORMATION



- + Quartz
- + Feldspar(s)
- + Magnetite
- + H<sub>2</sub>O

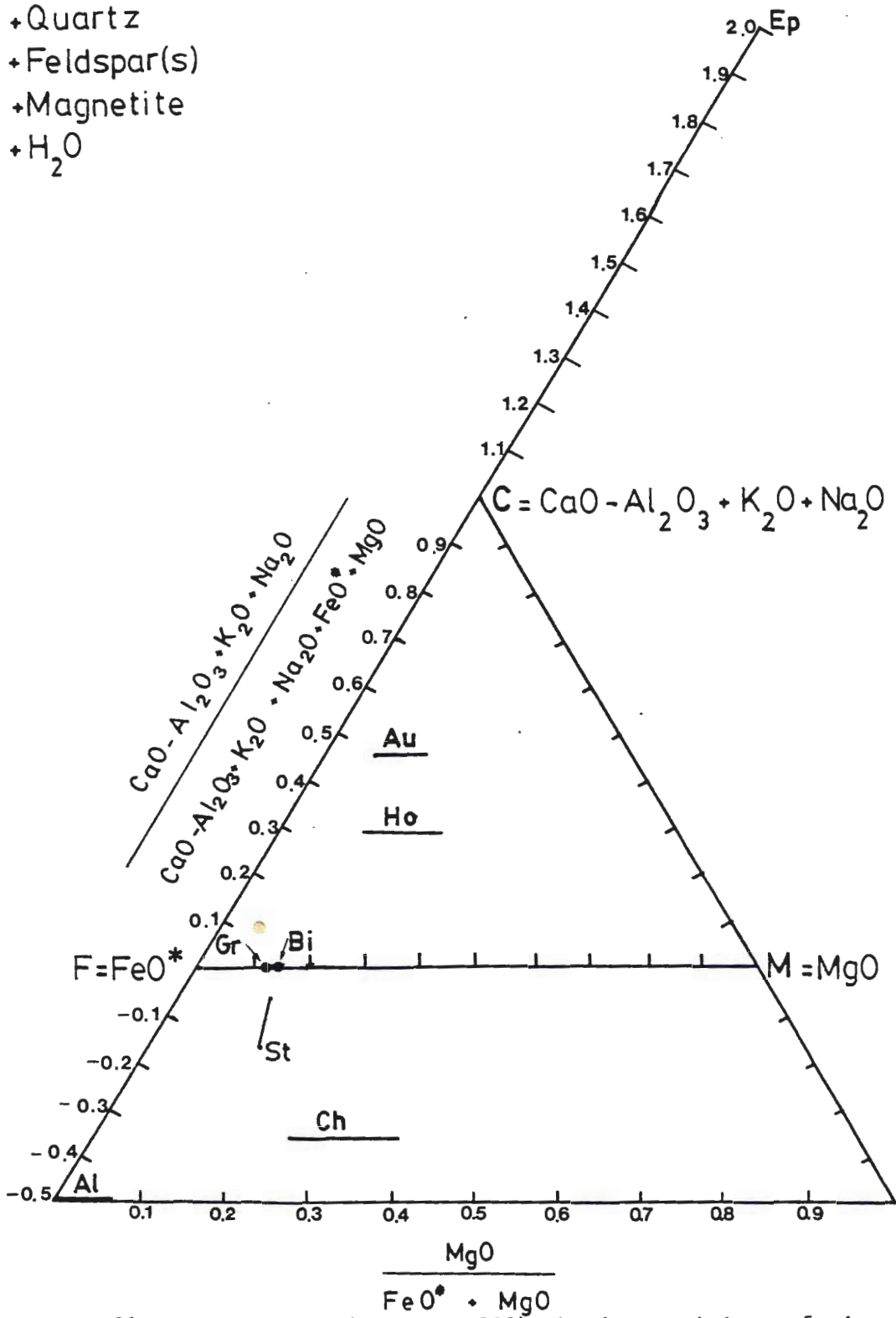


FIGURE 31: CFM diagram (Abbott, 1982) showing positions of minerals found in the metadiabase sill and the Negaunee Iron-Formation.

TABLE 5: PART A: EQUILIBRIUM ASSEMBLAGES OF THE METADIABASE

ZONE 1

au + bi + ho

au + ho + pl

au + ma + pl

ZONE 2

bi + ch + pl + ma

bi + ch + ho<sup>1,2</sup>

ho<sub>1</sub> + ma + pl

ZONE 3A

bi + ch + ho<sup>2</sup>

bi + ch + pl

bi + pl + ho<sup>1</sup>

bi + ho<sub>1</sub> + ma

ZONE 3B

al + bi + ch

ZONE 4

al + bi + ch

INTERCALATED CH. SCHIST

al + ch + gr

al + ch + ma + qu

bi + ch + gr

ch + gr + st + ma

al=almandine; au=augite; bi=biotite; ch=chlorite; gr=grunerite; ho<sub>1</sub>= first growth of hornblende; ho<sub>2</sub>=second growth of hornblende; ma= magnetite; pl=plagioclase; qu=quartz; st=stilpnomelane.

TABLE 5: PART B  
EQUILIBRIUM ASSEMBLAGES IN THE NEGAUNEE IRON-FORMATION

Arranged in order of stratigraphic position: The assemblage on the top line is present at the base of the formation. Multiple samples are arranged from left (base) to right (upper margin). All assemblages include quartz and magnetite.

bi + ch + gr + st (NI-8)

al + bi + gr (NI-7)

bi + gr + st (NI-7)

bi + gr + ho (NI-7)

bi + ch + st (NI-7)

ch + gr + st (NI-7, 6-180, 6-58, 6-5)

al + gr + st (NI-7, 6-58, 6-5)

al + ch + gr (NI-7, 6-5)

ch + gr + he (6-58, 6-5)

al + ch + st (6-5)

al=almandine, gr=grunerite, st=stilpnomelane, also see Table 1 for abbreviations of other minerals.

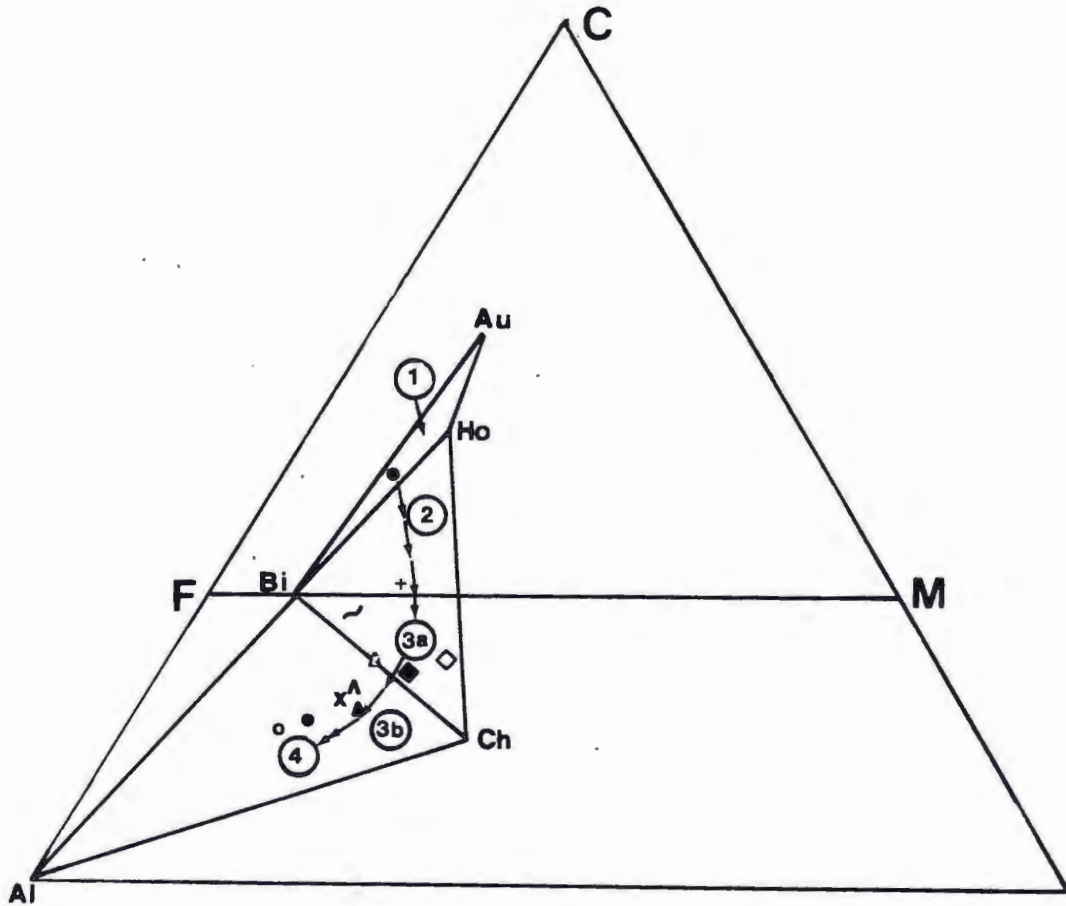


FIGURE 32: Equilibrium assemblages in the metadiabase sill. Circled numbers refer to zones of the sill. Bulk compositions correlated with the assemblage for each zone are also shown: Zone 1: ●=MD-26; Zone 3A: ◇ =6-238, ◆ =NM 10-5; Zone 3B: x=MWD-5, Δ =NM 10-13, Λ =E-3, ▲ =NM 10-11, ~ =6-204, + =6-201; Zone 4: ○ =6-180-C, ● =6-180-7. Succession of arrows indicate the changing direction of bulk composition through the four zones. Bulk compositions were calculated from whole rock analyses.

by an assemblage of bi- ch- ho which is compatible with the bulk compositions found in Zone 3A. The bulk compositions in Zone 3B and 4 are compatible with an assemblage of al- bi- ch. It is evident that the composition of the sill in Zone 3B favors the disappearance of plagioclase and hornblende and the appearance of almandine. The arrow on Figure 32 indicates the direction of changing bulk composition. This is compatible with Ca- depletion and Fe- enrichment produced by hydrothermal alteration. The assemblages are thus dependent on the bulk compositions found in the sill.

Modal analysis shows that epidote is present in only a few of the samples in the sill (Table 1). It may have developed by a late reaction of the form: hornblende  $\rightarrow$  chlorite + epidote (Abbott, 1984). (Hornblende is found pseudomorphed by these two minerals in sample MD-47). For these reasons it is not included in the assemblages shown in Figure 32.

The depletion of calcium moves the bulk compositions of the sill closer to the bulk compositions found in the iron- formation. Almandine is a minor mineral but is found in calcium- and sodium- depleted areas of the sill. Almandine probably developed at the contact of the sill and the Negaunee Iron-Formation by a reaction of the form:



Hsu (1968) suggests that such a reaction occurs between 550<sup>o</sup> and 600<sup>o</sup> C (at approximately 2 kbars) in the presence of a fayalite- magnetite- quartz buffer. Haase (1982) suggests that the area was subjected to pressures of 2-3 kbars and temperatures between 300-600<sup>o</sup> C. His results

indicate that reaction (1) could have occurred in this area.

Petrographic study of the Negaunee Iron-Formation indicates that the dominant minerals present are grunerite, magnetite, and quartz (Table 6). Almandine, biotite, chlorite, and stilpnomelane are minor minerals found throughout the iron-formation. Biotite is restricted to the base of the formation whereas stilpnomelane increases in abundance towards the upper section of the formation. All of the apparent equilibrium assemblages are plotted on the CaO-free area of the CFM diagram (Al<sub>2</sub>O<sub>3</sub> - FeO - MgO face) (Figure 33). This presents a problem of multiple crossing tie lines. The Gibbs Phase Rule is:  $f(\text{degrees of freedom}) = c(\text{components}) + 2 - p(\text{phases})$ . There are 5 phases (al- bi- ch- gr- st) and 3 components (Al<sub>2</sub>O<sub>3</sub>, FeO, MgO) present. The phase rule assumes that there is equilibrium ( $f > 0$ ). The number of phases is fixed so the problem may be resolved by the addition of a component ( $f = 4 + 2 - 5$ ; therefore  $f = 1$ ). This increases  $f$  to 1 suggesting that temperature can vary to equilibrate the system.  $F = 1$  is more realistic than  $f = 0$  because either pressure or temperature can vary. A potassic component is the obvious first choice. The resulting diagram is shown in Figure 35 and is derived from Figure 34. The mineral compositions used were determined by petrography, or XRD, and from analyses by Haase (1982). They are listed in Table 4 and shown in Figure 34. The Fe/Mg ratio for biotite was assumed to be equal to the Fe/Mg ratio of stilpnomelane and grunerite because they commonly replace each other and when they occur together are intergrown.

Both Table 5-B and Figure 35 show the succession of probable

TABLE 6: ESTIMATION OF MODES OF SELECTED SAMPLES  
FROM THE NEGAUNEE IRON-FORMATION

|         | <u>AL</u> | <u>BI</u> | <u>CA</u> | <u>CH</u> | <u>GR</u> | <u>HE</u> | <u>MA</u> | <u>QU</u> | <u>ST</u> |
|---------|-----------|-----------|-----------|-----------|-----------|-----------|-----------|-----------|-----------|
| NI-8    | 3         | 5         | -         | 5         | 12        | tr        | 40        | 30        | 3         |
| NI-7*   | 10        | 10        | -         | 5         | 53        | -         | 10        | 7         | 2         |
| D-5     | tr        | 3         | -         | 2         | 50        | -         | 25        | 20        | -         |
| D-6     | -         | -         | -         | 1         | 35        | -         | 15        | 48        | 3         |
| 6-180-B | tr        | -         | 3         | -         | 7         | -         | 25        | 65        | -         |
| 6-180-A | -         | -         | 5         | 7         | -         | 3         | 45        | 40        | tr        |
| 6-175   | 3         | -         | 10        | -         | 37        | 5         | 20        | 25        | -         |
| 6-145   | 5         | 5         | -         | -         | 40        | -         | 30        | 20        | tr        |
| 6-130   | -         | -         | -         | tr        | 5         | tr        | 40        | 52        | 3         |
| 6-65B   | 2         | -         | -         | 5         | 20        | 15        | 10        | 45        | 3         |
| 6-65A   | -         | -         | 2         | 3         | 15        | 7         | 13        | 53        | 7         |
| 6-58    | -         | -         | -         | 5         | 30        | 10        | 20        | 25        | 10        |
| 6-44+   | -         | 3         | -         | 3         | -         | -         | 54        | 40        | -         |
| 6-20    | -         | -         | -         | 10        | -         | -         | 40        | 43        | 7         |
| 6-5~    | 25        | -         | -         | 3         | 47        | 7         | 1         | -         | 15        |
| 6-0     | -         | -         | -         | 7         | 8         | 5         | 50        | 20        | 10        |

\* Also contains 3 % hornblende.

+ Also contains a trace amount of iron-talc.

~ Also contains 2% apatite.

Samples arranged from base to top of formation (from top to bottom of page).



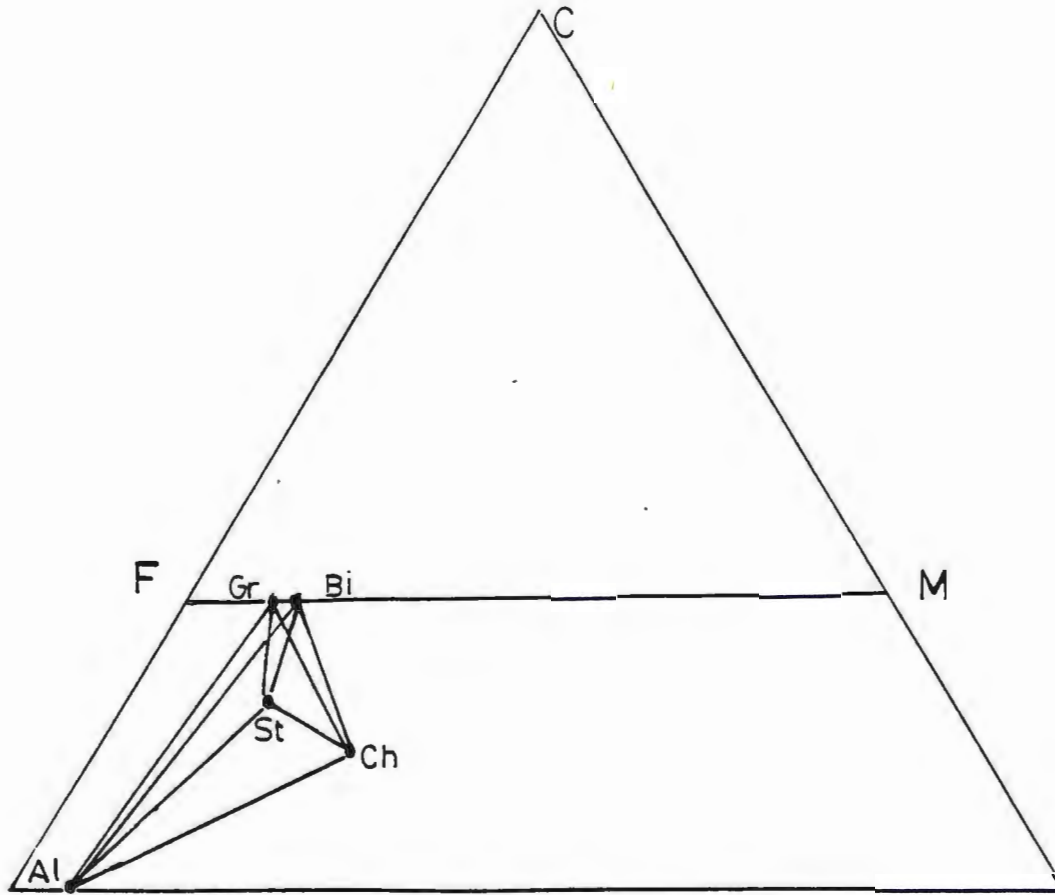


FIGURE 33: Equilibrium assemblages in the Negaunee Iron-Formation plotted on the CFM diagram. Note crossing tie lines.

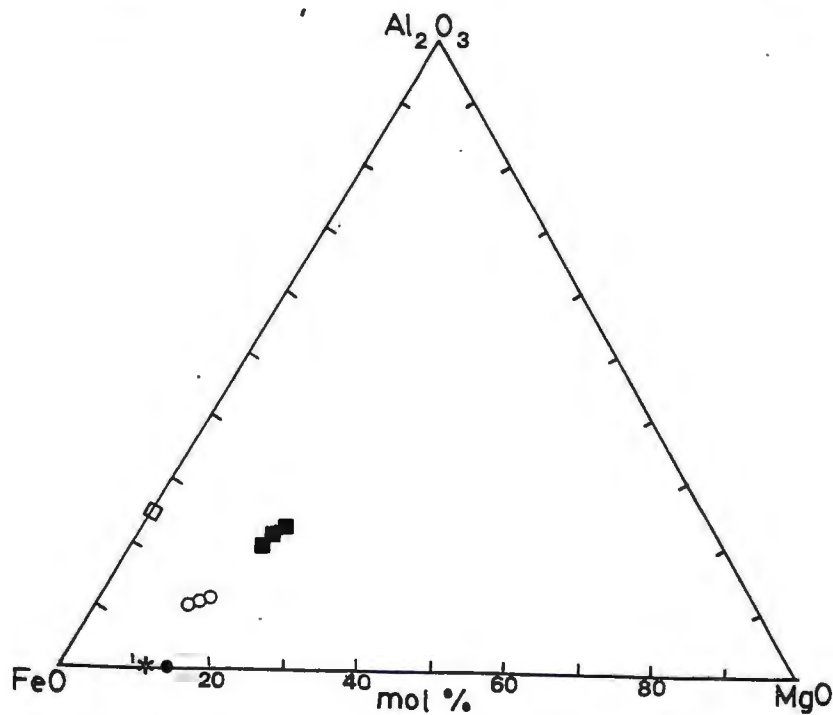
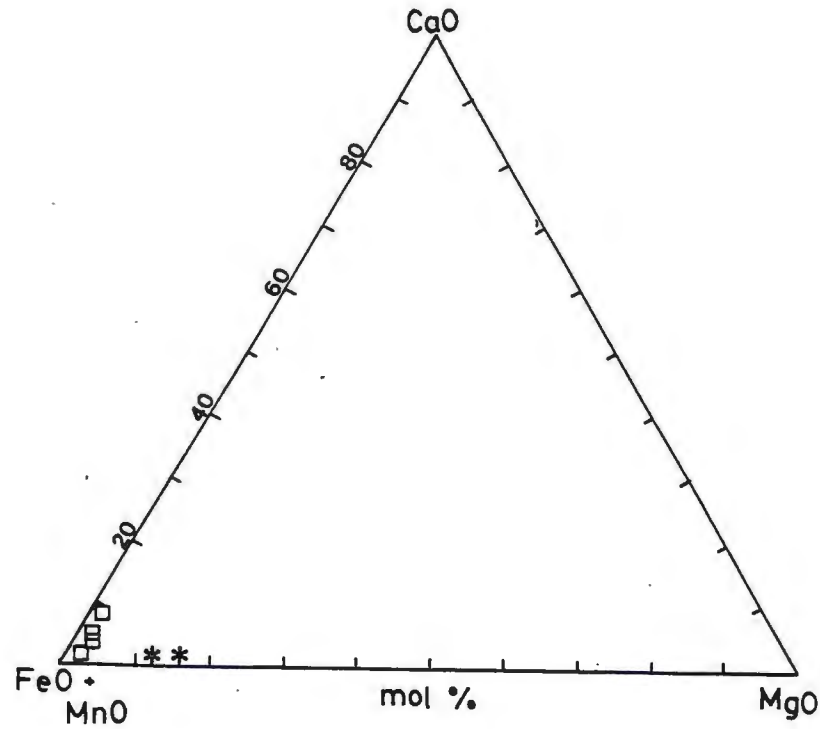


FIGURE 34: Compositions of minerals from Michigamme Mine. (Data isolated from Haase (1982) Figures 8 and 9).  $\square$ =almandine, \* =grunerite,  $\circ$ =stilpnomelane,  $\blacksquare$ =chlorite. (Biotite was assumed to have an Fe/Mg similar to stilpnomelane and grunerite, it was not analyzed by Haase at the mine,  $\bullet$ =biotite).

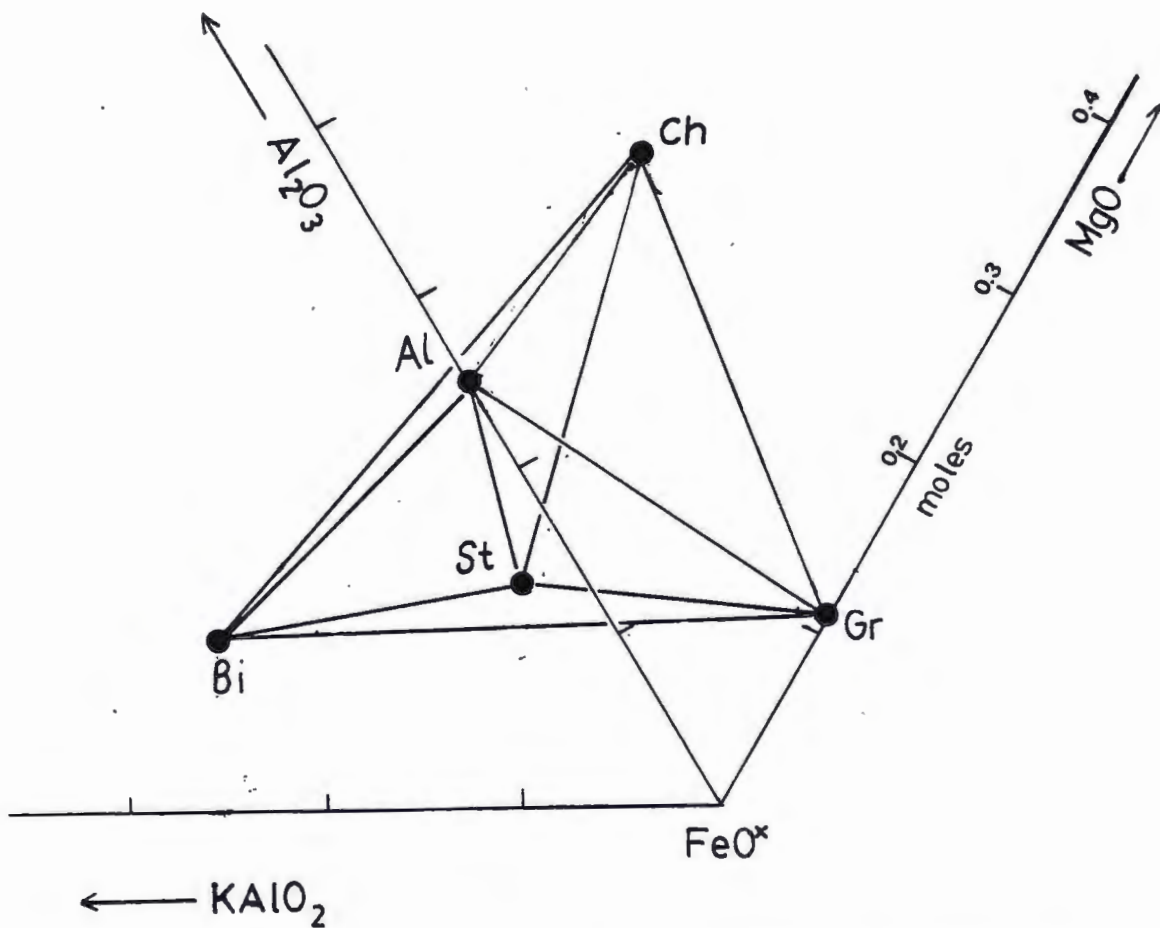
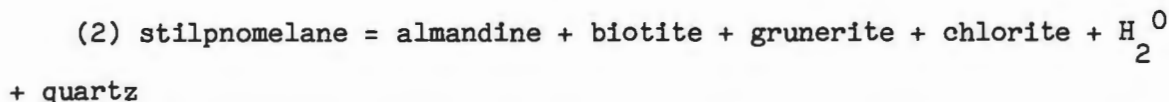


FIGURE 35: Equilibrium assemblages in the Negaunee Iron-Formation (some assemblages pertain to the chlorite schist, see Table 5A and 5B). From left to right, the 3-phase assemblages are shown as potassium is decreased: al-bi-ch; bi-ch-st, al-bi-st, al-ch-st; bi-gr-st, al-bi-gr, bi-ch-gr; al-gr-st, ch-gr-st, al-ch-gr. Note: Bi lies in the  $\text{KAIO}_2$ - $\text{FeO}^x$ - $\text{MgO}$  plane, at the base of the tetrahedron, and bi-st-gr are shown with the same Fe/Mg ratio, and st lies within the tetrahedron bi-gr-al-ch.

assemblages that are present as potassium is varied. Figure 35 also shows that a slight variation in Fe/Mg also may affect the succession of assemblages. These assemblages may have formed by a reaction of the form (with increasing temperature):



Possible equilibrium assemblages among the five phases al -bi -ch -gr -st include only one four-phase assemblage (bi -ch -gr -st), and all of the three- phase assemblages shown in Figure 35 except al-bi-ch and al-bi- st. Most of the samples from the iron- formation contain stilpnomelane. This, along with petrography (see p. 20), indicates that although reaction (2) may have been completed (as suggested by al -bi -gr and al -ch -gr ) it later reversed eliminating stable al- bi- ch- gr and developing stilpnomelane.

Chlorite schists intercalated with the iron-formation contain assemblages that contain the same mineralogy in different proportions as the iron- formation. It is the most iron- enriched part of the sill. The quantity of iron in the schist is probably similar to that in the iron- formation. The sill produces a different proportion of minerals because it started out with a different bulk composition and was initially chloritized.

#### SCENARIO

The Lake Michigamme area was part of a restricted subsiding basin during the Early Proterozoic (Larue, 1983). The Marquette basin is intracratonic yet an analogy is made to the modern ocean where sites of

hydrothermal activity occur at mid-ocean ridges. The metadiabase intruded into the Marquette basin in a deep-water setting. Fractures in the host iron-formation allowed fluids (from the Marquette basin) to penetrate to the upper margin of the sill and develop chlorite which recrystallized during regional metamorphism. Chlorite was formed because seawater lies in the chlorite and quartz stability field at 300°C in the system  $MgO - \frac{CaO-K_2O}{2} - \frac{Na_2O}{2} - \frac{Al_2O_3}{2} - SiO_2 - \frac{H_2O}{2}$  (Helgeson, 1967).

The chemical composition of the water in the Marquette basin may have been similar to modern seawater since the metadiabase - fluid interaction is analogous to modern basalt - seawater interactions. The major chemical exchange occurring during hydrothermal alteration is between  $Mg^{2+}$  from the water and  $Ca^{2+}$  from the rock. Experimental studies on salt solutions indicate that heavy metals such as Fe are rapidly leached from rocks interacting with the solution (Henley, 1983). A saline hydrothermal fluid could leach  $Fe^{2+}$  from the Negaunee Iron Formation which is in contact with the sill. The presence of  $Fe^{2+}$  in the hydrothermal fluid aids  $Mg^{2+}$  in forming chlorite. The amount of chlorite increases as the amount of  $Mg^{2+}$  exchanged increases but the presence of  $Fe^{2+}$  replaces some  $Mg^{2+}$  in forming chlorite (Mottl, 1983). When large quantities of  $Fe^{2+}$  are present, the fluid to rock ratio is actually greater than the value predicted in Figure 29 (< 30 for Zones 2, 3A; >50 for Zones 3B and 4). The fluid to rock ratios for the sill are greater than indicated by Figure 29 by at least a factor of 10 (Mottl, 1983) because of the presence of  $Fe^{2+}$ . The intercalated schist

responded to metamorphism as if it were an iron-formation which suggests that the Fe-enrichment in the sill is due to the iron-formation.

#### SUMMARY AND CONCLUSIONS

The stratigraphic sequence of the northern limb of the Marquette trough, from north to south, consists of the Siamo Slate, the Negaunee Iron-Formation, and the Goodrich Quartzite in the study area. The rock formations dip south. A diabase intruded along bedding (a zone of weakness) in the iron-formation and is found in contact with the slate in the northern part of the field area and the quartzite in the southern part of the field area. The metadiabase sill forms the topographic high in the area. The margins of the sill are finer-grained than the core, are laced with abundant quartz veins, and biotite and chlorite are foliated parallel to strike.

The quartzite of the Siamo Slate exhibits relatively constant grain size and mineralogy regardless of its distance from the contact with the base of the sill. The argillaceous schist of the Goodrich Quartzite exhibits a large concentration of chloritoid at its border with the sill suggesting that iron-enriched fluids passed from the sill into the schist.

The metadiabase was divided into 4 zones dependent on the degree of alteration. This was distinguished by the presence of relict poikilitic texture and the amount of chlorite present. A relict poikilitic texture of labradorite and augite located in Zone 1 is correlated with a relict poikilitic texture of plagioclase and hornblende which is present

through Zone 3A of the sill. Almandine, in Zone 3B, developed after hornblende became chloritized. The chlorite schist (Zone 4) contains an ellipsoidal texture which is traced from Zone 3B of the metadiabase. This texture is present in the schist regardless of whether it is a small body in the iron-formation or found between the iron-formation and the sill. The texture developed prior to the growth of almandine and grunerite. The Negaunee Iron-Formation is commonly brecciated and separated from the chlorite schist by almandine. Brecciation occurred prior to regional metamorphism because truncated magnetite granules are crosscut by grunerite. It dominantly consists of quartz, magnetite, and grunerite + almandine + biotite + chlorite + stilpnomelane. This assemblage is also found in the intercalated chlorite schist in different proportions.

The behavior of major elements across the sill is comparable to the behavior of major elements in several modern oceanic basalt-seawater alteration suites such as those described in Miyashiro and Mottl. FeO and MgO increase while  $\text{SiO}_2$ , CaO, and  $\text{Na}_2\text{O}$  all decrease in abundance with increasing degree of alteration. The sill is found in an intracratonic setting which differs from the midocean ridges, and the similar major element patterns are influenced by the influx of iron from the adjacent iron-formation. The mineralogy of the chlorite schist indicates alteration occurred in a strongly fluid-dominated system.

The major metamorphic mineral assemblages in the metadiabase sill change as the bulk composition of the sill changes towards the upper margin of the sill. The bulk composition of the sill controls the

spatial distribution of these assemblages which is most evident at the upper margin of the sill. Assemblages containing almandine are restricted to calcium- depleted and iron -enriched areas of the sill. This suggests that hydrothermal alteration preceded regional metamorphism. Hydrothermal fluids changed the bulk composition of the sill towards the bulk composition found in the iron- formation. The iron- formation aided the altering fluid in changing the bulk composition of the metadiabase before regional metamorphism occurred.



## REFERENCES

- Abbott, R.N., Jr. 1982. "A petrogenetic grid for high grade metabasites." *American Mineralogist*, 67, 865-876.
- \_\_\_\_\_. 1984. "The greenschist- amphibolite transition in the CFM projection." *American Mineralogist*, 69, 250-251.
- Cannon, W.F. and Klasner, J.S. 1972. "Guide to Penokean deformational style and regional metamorphism of the western Marquette range, Michigan:" *Field Trip Guidebook*, 18th Ann. Inst. on Lake Superior Geology, Houghton, Michigan, p. B1-B38.
- Fryer, B.J. 1977. "Rare-earth evidence in iron-formations for changing Precambrian oxidation states." *Geochimica et Cosmo. Acta*, 41, pp. 361-367.
- Gair, J.E. 1975. "Bedrock Geology and Ore Deposits of the Palmer Quadrangle, Marquette County, Michigan." U.S.G.S. Professional Paper 769. 159 p.
- \_\_\_\_\_ and Thaden, R.E. 1968. "Geology of the Marquette and Sands Quadrangles, Marquette County, Michigan." U.S.G.S. Professional Paper 397. 177 p.
- Haase, C.S. 1982. "Metamorphic Petrology of the Negaunee Iron Formation, Marquette District, Northern Michigan: Mineralogy, Metamorphic Reactions, and Phase Equilibria." *Econ. Geol.*, Vol 77, pp. 60-81.
- Haskin, L.A., Haskin, M.A., Frey, F.A., and Wildeman, T.R. 1968. "Relative and absolute terrestrial abundances of the rare-earths" in Origin and Distribution of the Elements (ed: L.H. Ahrens), pp. 889-912, Pergamon Press.
- Helgeson, H.C. 1967. "Solution chemistry and Metamorphism." in Researches in Geochemistry, P.H. Abelson (ed). v. 2. John Wiley and Sons, N.Y. pp. 363-394.
- Henley, R.W. and Ellis, A.J. 1983. "Geothermal Systems Ancient and Modern: A Geochemical Review." *Earth-Science Reviews*, 19, pp. 1-50.
- Hsu, L.C. 1968. "Selected phase relationships in the system Fe- Al- Mn- Si- O- H : A model for Garnet Equilibria." *Jour. Petrol.* v. 9, p. 40-83.
- James, H.L. 1955. "Zones of regional metamorphism in the Precambrian of northern Michigan." *GSA Bull.*, v. 66. no. 12. pp. 1465-1488. December 1955. *classic*

Klasner, J.S. 1978. "Penokean deformation and associated metamorphism in the western Marquette Range, northern Michigan." GSA Bulletin, v. 89, p. 711-722. May 1978. ✓

\_\_\_\_\_ and Cannon, W.F. 1974. "Geologic interpretation of gravity profiles in the western Marquette district, northern Michigan." Geol.Soc. Am. Bull. 85, pp. 213-218.

\_\_\_\_\_ 1978. "Bedrock Geologic Map of the Southern part of the Michigamme and Three Lakes Quadrangles, Marquette and Baraga Counties, Michigan." U.S.G.S. Miscellaneous Investigations Series. Map I-1078. ?

Klein, C. and Hurlbut, C.S., Jr. 1985. Manual of Mineralogy, 20th edition, J. Wiley & Sons, New York.

Larue, D.K. 1983. "Early Proterozoic tectonics of the Lake Superior region: Tectonostratigraphic terranes near the purported collision zone." GSA Memoir 160. pp. 33-46.

Miyashiro, A; Shido, F.; and Kanehira, K. 1979. "Metasomatic chloritization of gabbros in the Mid-Atlantic Ridge near 30°N." Marine Geology, Vol 31, No. 1/2, April 1979, pp. M47-M52.

Mottl, M.J. 1983. "Metabasalts, axial hot springs, and the structure of hydrothermal systems at mid-ocean ridges." GSA Bull. v. 94 pp. 161-180. (February).

Rose, W.I., Bornhorst, T.J., and Sivonen, S.J. 1985. "Rapid, High Quality Major and Trace Element Analysis of Powdered Rock by X-ray Fluorescence Spectrometry (in press)." Xray Spectroscopy.

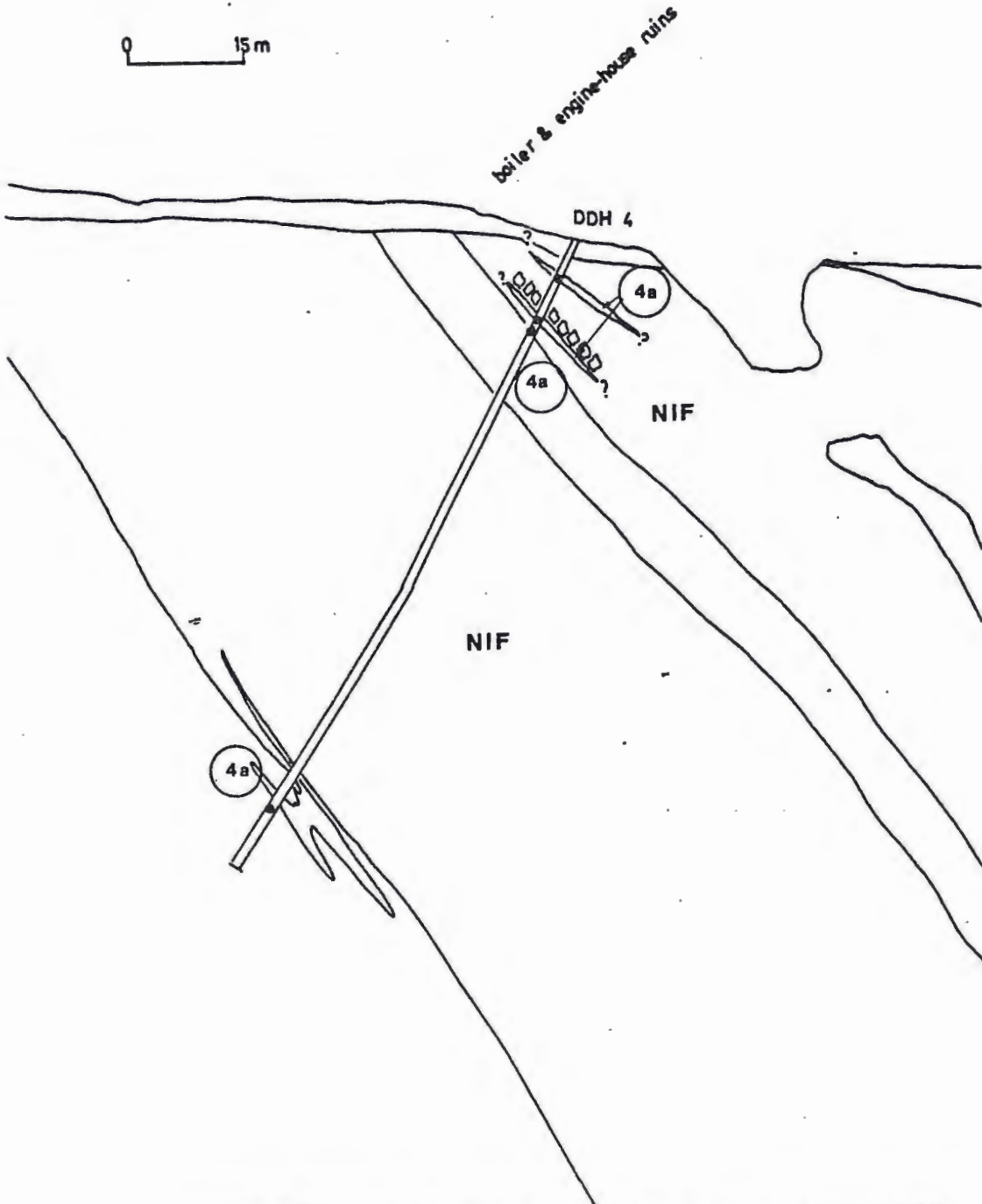
Veblen, D.R. and Ribbe, P.H. (eds). 1982. "Amphiboles: Petrology and Experimental Phase Relations." Reviews in Mineralogy. Volume 9B, Mineralogical Society of America. p. 121.

A P P E N D I X A

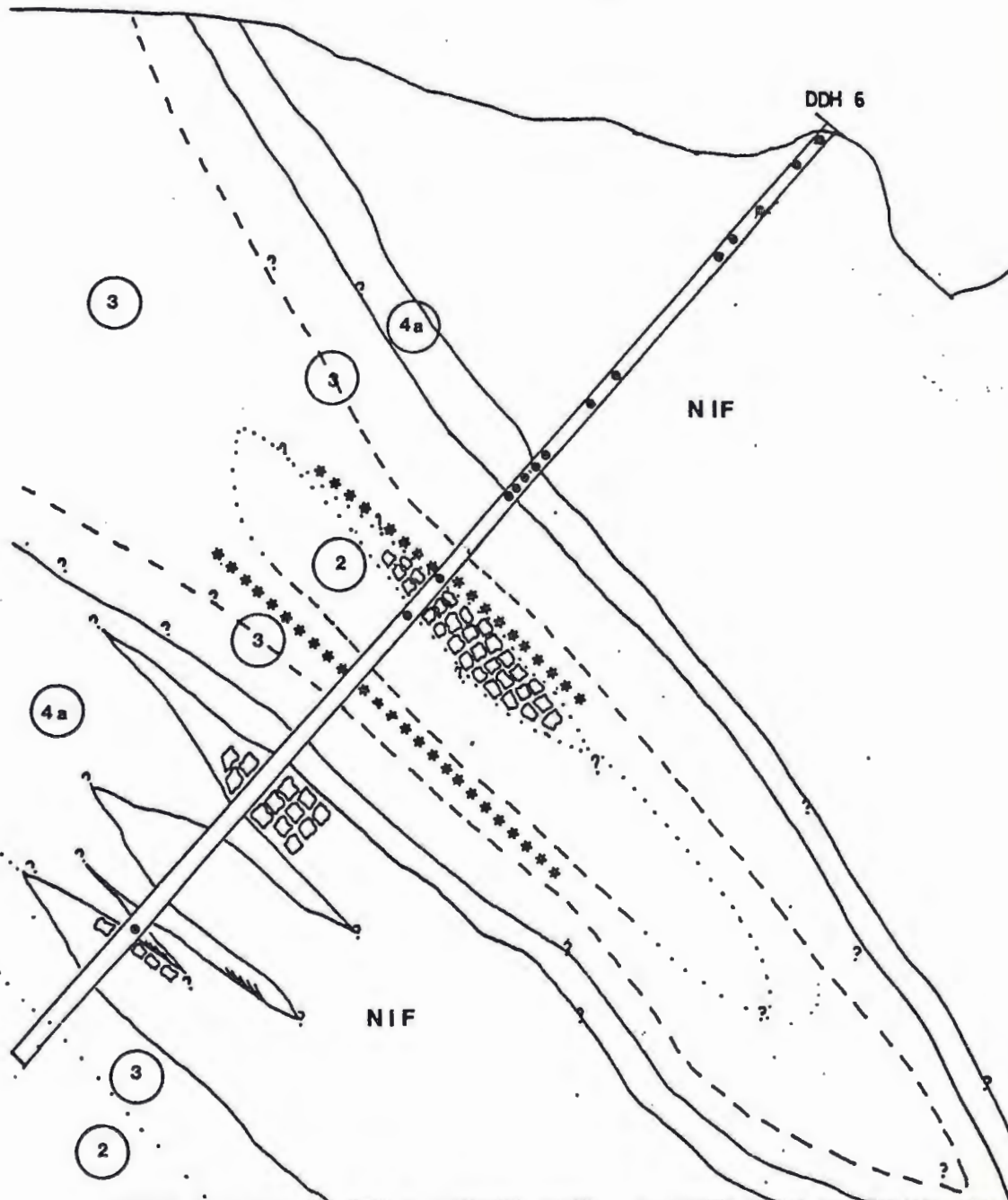
CROSS-SECTIONS OF DDH 4 AND 6

0 50 ft

0 15 m



CROSS-SECTION OF DDH 4 SHOWING SAMPLE LOCATIONS (•) AND INFERRED GEOLOGY. LOOKING EAST. SEE PLATE 1 FOR LEGEND. ADAPTED FROM CLEVELAND CLIFFS IRON COMPANY EXPLORATION CROSS-SECTION. □ = BRECCIA-TION. NIF= NEGAUNEE IRON -FORMATION.



CROSS-SECTION OF DDH 6 LOOKING EAST. ADAPTED FROM CLEVELAND CLIFFS IRON COMPANY EXPLORATION CROSS-SECTION. ●=SAMPLE LOCATION. □ = BRECCIATION. \* = STRIATIONS. NIF=NEGAUNEE IRON-FORMATION. SEE PLATE 1 FOR LEGEND.